Geophys. J. Int. (1990) **101**, 181–202

The strain pattern in the western Hellenic arc deduced from a microearthquake survey

D. Hatzfeld,[1] G. Pedotti,[1] P. Hatzidimitriou[2] and K. Makropoulos[3]

[1] *Observatoire de Grenoble, IRIGM, BP53X, 38041 Grenoble Cedex, France*
[2] *Geophysical Laboratory, Aristotelian University, PO Box 352-1, 54006 Thessaloniki, Greece*
[3] *Department of Geophysics, University of Athens, 15784 Ilissia, Athens, Greece*

Accepted 1989 October 23. Received 1989 June 20

SUMMARY

More than 1000 earthquakes recorded during 7 weeks in 1986 in the Peloponnese and surrounding areas show shallow seismicity spread over a wide area bounded by the Hellenic trench. The highest level in the energy release is for clusters located along the Hellenic trench, where changes in the morphology are seen. A few clusters are also observed, as at the intersection between the Gulf of Corinth and the Gulf of Patras, near the Lake Trikhonis, or between Kythira and Crete. In the Peloponnese, the shallow earthquakes do not define single faults, but are diffusely distributed. A higher concentration and a deepening of the foci (within the whole crust) towards the west seem to reflect a higher strain rate there. Fault plane solutions exhibit a scattered pattern for earthquakes shallower than 11 km, but for earthquakes deeper than 11 km, they show some consistency in the orientation of *P*-, *T*-, and *B*-axes. Gently dipping nodal planes are seen all over the Peloponnese, with the conjugate vertical plane striking in various directions, and with no consistency in the sense of motion. These earthquakes are located between 8 and 18 km deep and could reflect a decoupling between the lower and the upper crust. Reverse faulting is seen in the Gulf of Kefallinia and the western Peloponnese. The *P*-axes trend NE–SW to E–W. Normal faulting is seen in the Gulf of Corinth and in central Peloponnese with the *T*-axes trending N–S, and in the southern Peloponnese, where the *T*-axes trend NW–SE. The deformation over the western Hellenic arc, revealed by fault plane solutions of earthquakes with depth between 11 and 40 km, appears to be the superposition of two phenomena. First, throughout the Aegean, crustal extension with orientation roughly parallel to the trench dominates, with crustal shortening and subduction along the Aegean arc. Superimposed on this is a more local effect of the collision between the Aegea and Apulia which seems to induce horizontal compression roughly perpendicular to the Aegean arc west of the Peloponnese and Epirus. The compression due to this decays eastward, at a distance comparable with the width of the collision zone. The deepening of the brittle–ductile transition is likely to be due to an increase of the strain field towards the Ionian islands.

Key words: continental deformation, Hellenic arc, seismotectonics.

INTRODUCTION

This paper is concerned with the seismotectonics of the western Hellenic arc, which includes the Ionian islands, the Peloponnese and the Kythira strait (Fig. 1).

The geodynamics of the Aegean area is probably the most complex of the Mediterranean: the Aegean 'plate' is located between the European and the African lithospheric plates, whose relative motion is convergent in a N–S direction, with a velocity of about 2 cm yr^{-1} (Minster & Jordan 1978). The relative motion between the southern edge of Aegea and Africa, across the Hellenic trench, however, is of about 7–10 cm yr^{-1} in a NE–SW direction (McKenzie 1972, 1978; Le Pichon & Angelier 1979; Jackson & McKenzie 1988). In contrast, the geological framework of the western Hellenic arc, inherited from tectonic episodes of the upper Eocene–Oligocene time, shows the thrusting of the Hellenic

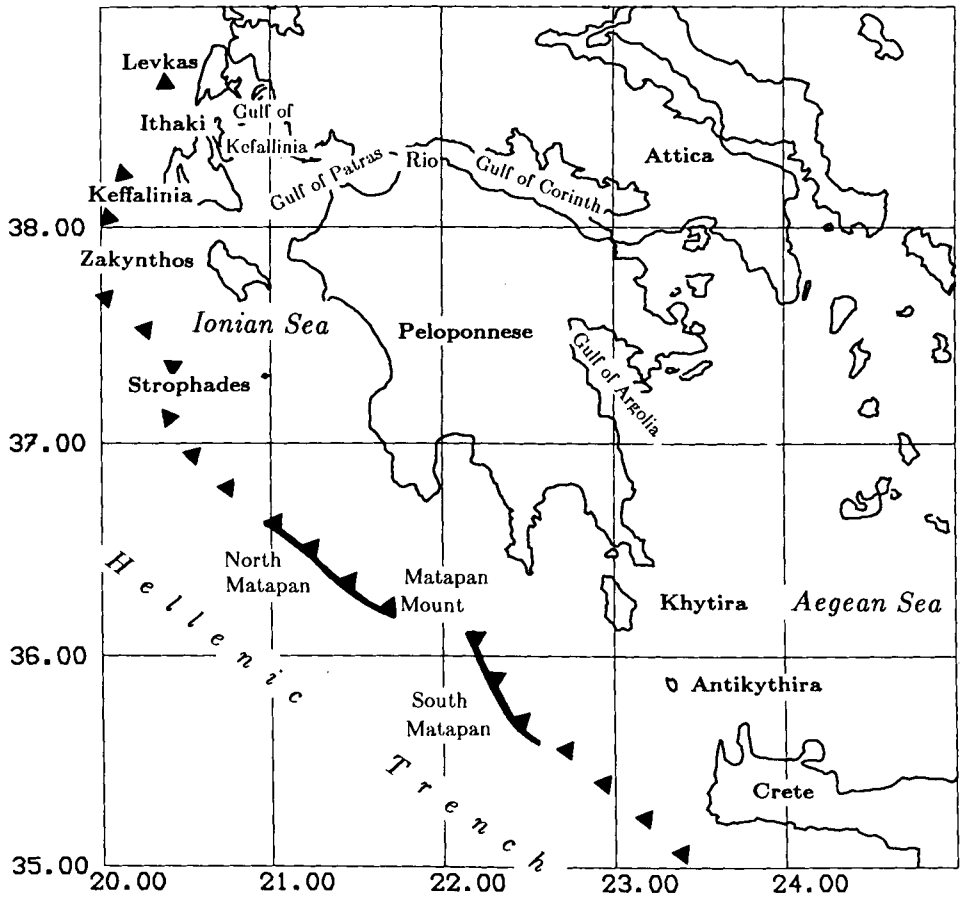

Figure 1. Map of the western Hellenic arc. The main features of the bathymetry after Le Quellec *et al.* (1980) are represented by a continuous barbed line when they are clear and triangles when they are less clear.

nappes (Ionian and Gavrovo) over the stable Preapulian zone along NW–SE front (Aubouin 1959).

Since upper Miocene time, important changes in the tectonics caused extensional basins to develop within the internal Aegean area (Mercier *et al.* 1979; Le Pichon & Angelier 1979). This time is thought to be the beginning of the subduction of the lithospheric African plate beneath the Aegea, at the Hellenic trench, a clear feature in the bathymetry west of the Peloponnese, but not as clear northward, west of Ionian islands (Le Quellec *et al.* 1980).

Detailed neotectonic studies (Mercier *et al.* 1979; Sorel 1976; Sébrier 1977; Angelier 1979; Lallemant, Lyberis & Thiebault 1983) over the Ionian islands, the Gulf of Corinth and the Peloponnese, show a complex strain pattern for Quaternary time: E–W compression in the external part of the Hellenic arc (i.e. the Ionian islands), but N–S extension around the Gulf of Corinth and E–W extension in the southern Peloponnese and western Crete.

The shallow seismicity clearly defines the Hellenic arc from Corfu to Rhodos. The deepening of the earthquakes towards the internal Aegean (Papazachos & Comninakis 1971; Makropoulos & Burton 1981) is associated with the subducted slab. Shallow seismicity is also spread over most of the Aegean area with concentration in some places, such as the Gulf of Corinth, and the western Peloponnese. However no clear individual faults can be mapped from the seismicity, even in the Gulf of Corinth, where several earthquakes occurred in 1981, several faults slipped. The western Hellenic arc has experienced several strong earthquakes during the past decade, in the Gulf of Corinth, the Ionian islands, and in Kalamata.

The only reliable fault plane solutions, determined from the World-Wide Standardized Seismograph data (e.g. McKenzie 1972, 1978; Jackson, Fitch & McKenzie 1981; Jackson *et al.* 1982; Papazachos *et al.* 1988; Lyon-Caen *et al.* 1988), clearly show compression in the external part of the Hellenic arc, but N–S extension in the Gulf of Corinth and E–W extension from the southern Peloponnese to Crete.

We were interested in understanding better the tectonics of the western Hellenic arc, from the Gulf of Corinth to Crete, where a non-uniform strain pattern has been inferred (Le Pichon & Angelier 1979; Lyberis & Lallemand 1985; Mercier *et al.* 1987). The spacing between the permanent stations, in this area, does not allow precise location or the determination of individual focal mechanisms. Data from the WWSSN are not precise enough because of the strong lateral heterogeneity in the velocity structure. If the spacing between the stations is reasonably small, this should allow one to locate the earthquakes with a good accuracy and compute individual fault plane solutions. But the question of relating the information obtained from small earthquakes during a short period of time to geodynamical process will remain. In order to bring more detailed information about the tectonics of the western Hellenic arc, in the summer of

1986 we installed a dense network of 46 temporary stations and conducted a microearthquake survey during 7 weeks. This paper describes the results obtained for shallow seismicity. Another paper (Hatzfeld *et al.* 1989) is concerned with the results concerning the subduction zone.

DATA ACQUISITION AND EARTHQUAKES LOCATION

The seismograph network (Fig. 2) was designed to cover the western termination of the Hellenic arc, including the Ionian islands, the Peloponnese, the Gulf of Corinth and the islands of Kythira and Antikythira. The stations were visited every 2 days in order to change the records, make time corrections, and check the instruments. Readings of the 650 seismograms gathered were made using a magnifying lens, and we assume a total uncertainty in time smaller than 0.2 s for P and 0.5 s for S arrival times (Pedotti 1988). The 1070 earthquakes recorded by a minimum of five stations were first located (Fig. 3) using the HYPO71 routine (Lee & Lahr 1972), and a simple velocity structure (Makris 1978).

The next steps were to estimate the V_P/V_S ratio and improve the velocity structure, and the final step was to estimate the absolute and relative uncertainties in the earthquake locations (Pedotti 1988). We divided the studied area into three different regions, according to the tectonics and the inferred velocity structure: region 1 is the Gulf of Corinth, region 2 is the Peloponnese, and region 3 is the Ionian sea.

1 The V_P/V_S ratio

The V_P/V_S ratio, which can vary from 1.65 to 1.80 depending on the area, is an important parameter for the depth control of the earthquakes.

First, we constructed individual Wadati plots for all the events having more than five S arrival times. As usual, the scatter is large for ratios obtained with only five readings, but a mean V_P/V_S ratio of 1.79 ± 0.02 was found using 97 earthquakes, and we did not observe a difference between three different regions.

Second, we plotted, for all the earthquakes, the differences in P arrival times ($tpi - tpj$) versus the differences in S arrival times ($tsi - tsj$) at pairs of stations. This method allows us to use more data and smooth the results. For the Gulf of Corinth, we obtained a mean $V_P/V_S = 1.797 \pm 0.003$, which is close to the value found by King *et al.* (1985) in the same era. For the Peloponnese, the mean V_P/V_S ratio was found to be 1.773 ± 0.004, and 1.763 ± 0.006 for the Ionian sea.

2 The velocity structure

We do not know the detailed velocity structure in this area. Seismic refraction profiles (Makris 1978) and traveltimes for *Pn* phases (Panagiotopoulos & Papazachos 1985) are consistent with a crustal thickness of 45 km in the Peloponnese, but only 20 km beneath the Ionian islands, with this crust overlying a mantle with a velocity of about

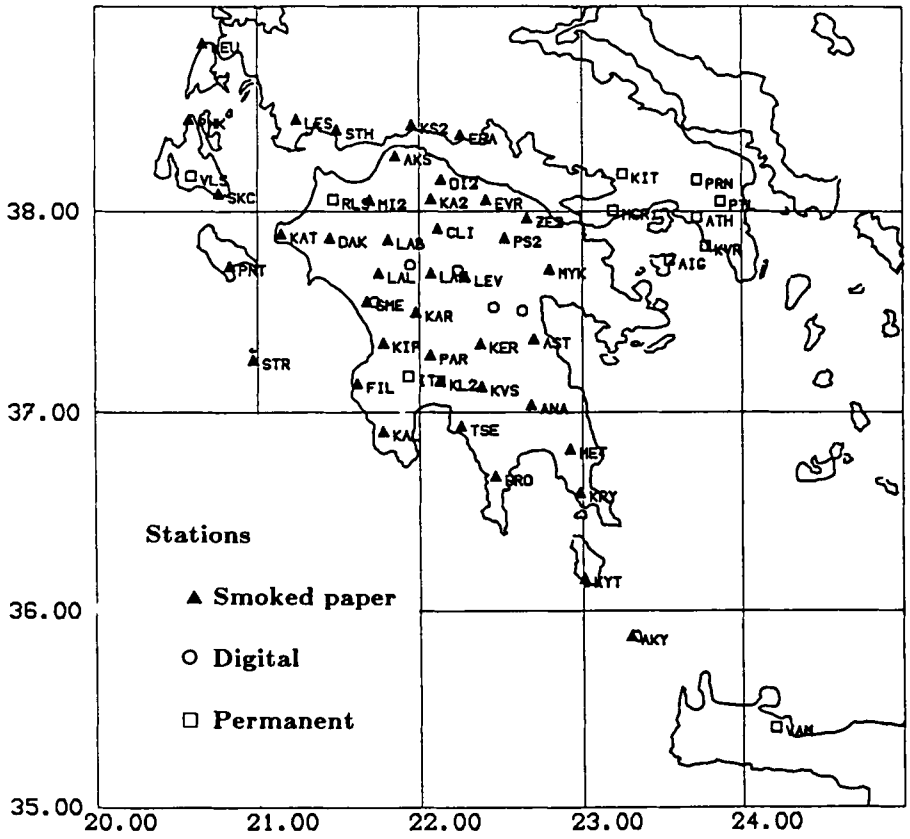

Figure 2. Map of the seismological stations installed during the experiment.

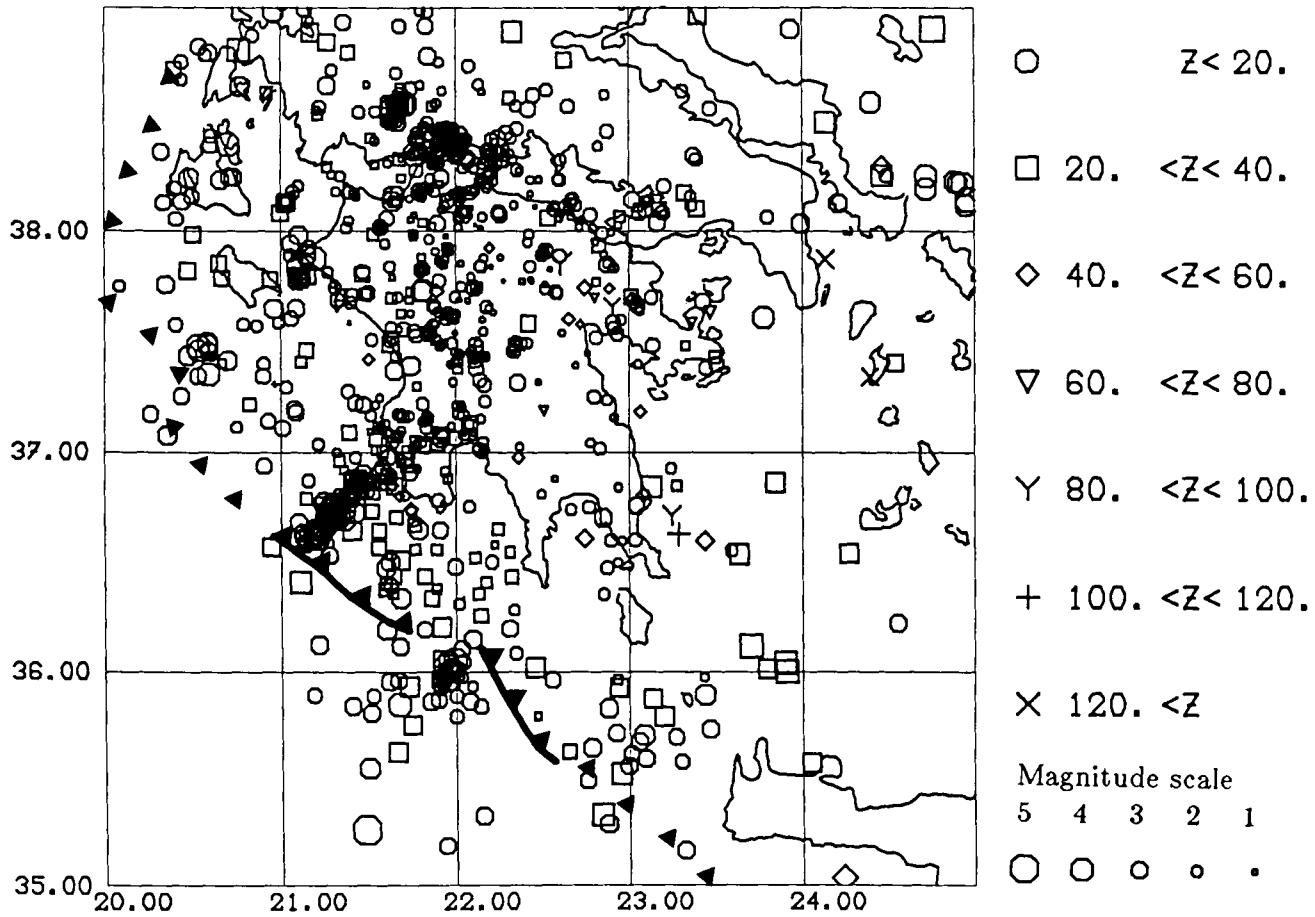

Figure 3. Seismicity map of all the 1070 events located from 1986 June 6 to 1986 July 17. The different symbols represent different depths and the size of the symbol indicates the magnitude of the event.

7.7 km s^{-1}. This is a rough estimate of the velocity, which is not precise enough to yield accurate locations of the earthquakes.

In a first step, to determine a more refined velocity structure, we selected 56 events for the Gulf of Corinth, 62 for the Peloponnese, and 59 for the Ionian sea recorded by a minimum of 15 stations. We plotted the traveltimes versus the epicentral distance. Because we used earthquakes, there is a trade-off between the location and the traveltime. Moreover, using only first arrivals, we do not sample all the layers. Therefore this method is useful only for approximating the mean velocity for the whole crust and the mantle. For the three regions, and for crustal events both shallower and deeper than 20 km, we obtained the same value of $V_c = 6.00 \pm 0.02$ km s^{-1}. For the mantle velocity, we used waves refracted beneath the Moho, and obtained a mean value of $V_m = 8.0 \pm 0.2$ km s^{-1}.

Second, in each region we located the selected events using several tens of velocity structures including one, two or three layers of different velocities for the crust and an overlying half-space, and examined the traveltime residuals. The mean rms minimization yielded to the same structure for regions 1 and 2, but a slightly different one for region 3 (Table 1). The relatively thicker crust found in model 3, in apparent contradiction with the velocity structure found by Makris (1978) and Panagiotopoulos & Papazachos (1985), is likely to be due to the use of *Pn* phases which do not allow a precise determination of the model.

3 Precision in the locations

There are two main causes of mislocations of the earthquakes. The first is due to noise present in the data, which is introduced mainly by errors in the readings, time

Table 1. Velocity structures for models 1–3.

Model 1		Model 2		Model 3	
Velocity (km/s)	Depth	Velocity (km/s)	Depth	Velocity (km/s)	Depth
5.9	0.	5.8	0.	6.0	0.
6.3	15.	6.0	10.	8.0	45.
8.0	40.	6.4	20.		
		8.0	40.		

corrections, and location of the stations. These errors can be estimated from the covariance matrix in the HYPO71 routine, which gives us parameters rms (root mean square traveltime residual), ERH and ERZ (horizontal and vertical error in location). We decided to keep only the earthquakes recorded with a minimum eight *P* and one *S* arrival time, an rms value smaller than 0.5 s, and ERH and ERZ values smaller than 5 and 10 km, which gives us two different data sets.

The second cause of mislocation can be due to systematic bias (for instance local effect or inaccurate velocity structure). These errors are much more difficult to estimate. It is not possible to conduct realistic synthetic tests because there is a strong influence of the noise of the data on these systematic bias, and there is no way to keep all the well-located events and eliminate all the poorly located events (Grange *et al.* 1984; Hatzfeld *et al.* 1986).

Our final goal is to keep only the earthquakes whose locations are uncertain by less than 5 or 10 km. To achieve this goal, we located all the earthquakes that passed the statistical tests described above, using different realistic velocity structures, and kept only those whose epicentres, and depths differ by less than 5 and 10 km, from those located with the different velocity structures found previously (Table 1) and that given by Makris (1978). Thus, even if we are not sure that we know the real velocity structure, we can trust the locations of our earthquakes.

The magnitudes of the earthquakes were estimated using the HYPO71 formula (Lee & Lahr 1972). This formula, which uses the signal duration, has been established empirically for California. Therefore the estimate of the magnitude is not very accurate.

RESULTS

Applying these criteria left us with 671 earthquakes located better than 10 km and 437 earthquakes better than 5 km, both in epicentre and depth (Fig. 4).

We computed fault plane solutions for 80 shallow earthquakes, for which more than 12 polarities were available and the gap in azimuth was smaller than 90° (see the Appendix and Table 2). For a few specific areas, we could not fulfill these criteria, but we wanted to look for possible consistency with the general pattern deduced from the fault plane solutions. We therefore relaxed some of the criteria. The corresponding solutions are listed separately in Table 2.

General description

As pointed out in Pedotti (1988) and Hatzfeld *et al.* (1989), the seismicity is spread over a wide area and no individual fault can be clearly seen. The level of seismicity is higher towards the west and is bounded by the Hellenic trench.

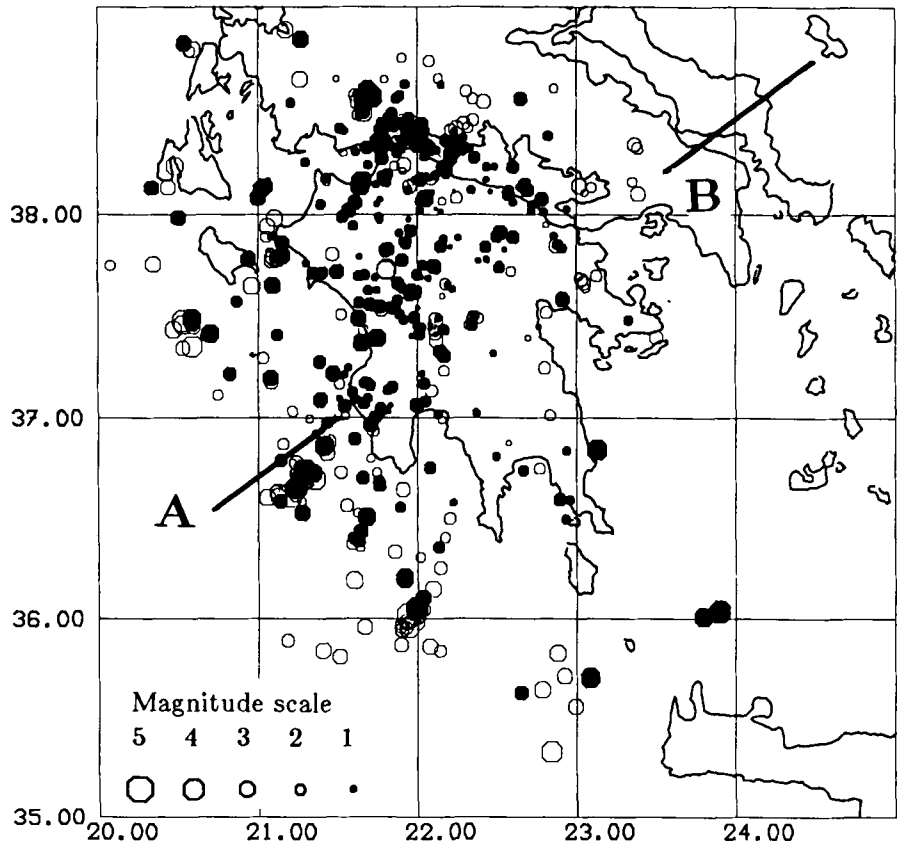

Figure 4. Seismicity map of the well-located events. The empty dots are the 671 earthquakes located with an accuracy better than 10 km (the black dots are the 437 events located with accuracy better than 5 km). Notice the clusters along the Hellenic trench and the decrease of seismic activity towards the eastern Peloponnese. A–B is the location of the cross-section shown in Fig. 5(b).

Table 2. Parameters of the fault plane solutions.

Nb	Date & Time	Lat °N	Long °E	Z km	Mag	Plan1		Plan2		P Axis		T Axis	
						As	Pl	As	Pl	As	Pl	As	Pl
73	860609 9:59	37.69	21.73	38.1	1.3	300	50	120	39	209	85	30	5
99	860610 8:48	37.91	21.88	10.2	1.3	280	40	40	67	154	15	267	54
103	860610 13:15	38.17	21.42	6.9	1.8	280	50	40	59	255	54	158	5
119	860611 6:55	37.90	22.51	15.3	2.1	300	10	80	82	175	36	342	52
123	860611 8:21	37.63	21.68	28.2	1.5	180	60	0	29	269	15	90	75
124	860611 8:25	37.63	21.68	29.1	1.6	40	50	280	59	244	54	341	5
158	860612 4:47	38.37	21.94	11.2	1.9	100	70	260	21	21	64	184	24
167	860612 8:31	37.43	22.16	15.9	1.4	110	20	290	70	199	65	19	25
173	860612 13: 0	37.30	22.17	18.2	2.4	260	90	250	0	170	45	350	45
174	860612 13:44	37.50	22.38	12.6	1.5	200	60	70	41	60	61	311	9
209	860613 15:21	38.02	21.56	21.4	1.5	270	50	90	39	180	85	0	5
210	860613 15:23	38.02	21.56	20.9	2.7	310	40	160	53	236	7	121	73
212	860613 16:11	37.94	21.59	18.3	1.7	170	30	40	69	113	21	341	59
221	860613 23:25	37.46	21.99	11.8	1.5	170	20	70	86	142	38	359	45
315	860615 19:21	38.37	21.79	6.3	2.6	270	30	90	59	0	75	180	14
319	860615 22: 6	37.74	22.51	11.1	1.9	40	40	140	81	14	40	259	26
322	860616 1:46	37.85	21.13	19.5	2.6	180	10	80	88	0	45	160	42
345	860616 16:19	37.46	22.09	9.0	1.8	100	50	0	78	311	36	55	18
352	860617 2:52	38.15	21.67	28.4	1.9	190	50	20	40	284	4	58	83
353	860617 3: 4	38.14	21.65	26.0	2.0	230	90	140	90	95	0	5	0
358	860617 6:42	37.75	22.03	10.0	1.7	280	80	188	78	144	15	53	0
380	860617 23:39	37.63	21.76	8.0	1.2	225	75	320	71	182	23	272	2
390	860618 11:24	37.43	22.16	15.6	1.3	210	60	29	30	120	75	299	15
402	860618 14: 6	37.49	22.35	10.7	1.3	210	50	19	40	295	4	161	83
418	860619 2: 7	37.56	21.60	20.8	2.0	170	40	340	50	74	5	211	82
430	860619 5:45	37.54	21.83	32.5	1.7	250	50	110	47	92	68	359	1
431	860619 5:52	37.54	21.84	31.1	2.2	220	88	40	1	310	43	130	47
481	860620 3:40	38.13	21.03	25.4	2.7	280	60	140	37	26	12	146	66
482	860620 3:55	38.12	21.02	29.1	2.8	295	60	130	30	30	14	185	73
493	860620 12: 4	38.13	21.04	23.9	2.6	250	22	60	68	152	23	323	66
504	860621 2:12	38.33	22.07	13.6	2.2	280	60	169	59	135	45	44	0
509	860621 6:52	38.32	22.05	9.3	2.5	310	60	60	59	274	45	5	0
515	860621 14:22	37.37	21.63	12.6	3.2	275	15	60	77	157	32	319	56
516	860621 17: 4	37.46	22.34	8.4	2.2	340	10	160	80	250	35	70	55
535	860622 7:23	37.49	21.62	23.0	2.9	190	70	60	29	296	21	68	58
560	860622 22: 6	37.63	21.90	12.1	1.8	160	10	340	80	69	35	249	55
573	860623 14:31	38.50	21.64	1.2	3.1	240	48	35	44	317	1	220	77
585	860623 21:23	38.06	21.59	22.2	2.6	40	30	310	90	246	37	13	37
588	860623 21:55	38.33	21.68	36.1	2.3	220	70	330	46	174	46	280	14
613	860624 22: 4	38.35	21.77	16.9	4.1	290	80	20	90	245	7	154	7
614	860624 22:12	38.36	21.78	12.4	2.8	210	60	0	33	155	70	288	13
637	860625 18:33	37.71	21.49	22.5	2.4	150	40	330	49	59	5	239	85
649	860626 2:56	38.26	21.92	17.7	2.8	180	70	310	29	121	58	253	21
667	860626 14:20	37.39	22.10	13.3	2.7	200	30	70	69	11	59	143	21
677	860626 21:48	37.91	22.52	12.2	2.6	180	10	272	89	172	44	11	43
694	860627 5:30	38.34	22.07	13.0	2.8	0	60	240	49	216	54	117	6
718	860628 2:57	37.96	21.09	9.3	3.2	30	80	300	90	254	7	345	7
720	860628 4:37	37.62	21.98	15.8	2.2	30	70	290	64	251	33	159	3

Intermediate depth events are located in the eastern part, beneath the Gulf of Argolia, but there are not many earthquakes deeper than 40 km, which we found surprising (Hatzfeld *et al.* 1989).

A few dense clusters are seen in some places and will be described in greater detail below: along the Hellenic trench, with the Gulf of Patras and the Gulf of Corinth, between the Peloponnese and Crete. The number of earthquakes cannot be related directly to strain, because we have to take into account the magnitude of the events. We plotted on Fig. 6 a map of the energy released by the earthquakes. We used the method of the moving block (Bath 1982), the size of the block being 40 km. This map applies to a period of only 6 weeks but it allows us to locate better the concentration of brittle deformation. This map shows a pattern slightly different from the seismicity map: the most active zones are located in the Ionian sea (along the Hellenic trench) and in the Kythira strait, where the crust is probably thinner. These observations agree with those of Makropoulos (1978) and Hatzidimitriou (1984). The western Peloponnese is more active than the eastern part, and we observe an active cluster of seismicity around the Rio located between the Gulf of Corinth and the Gulf of Patras.

An examination of the depths shows that the events are located within the whole of the crust, and not just in the upper part of it. A histogram of the depth of the events for the Peloponnese (Fig. 5a) shows that the depths range from the surface to 40 km with a maximum around 15 km. A cross-section (Fig. 5b) shows clearly that the deepest crustal events are located in the western part of the Peloponnese. This observation is in agreement with the results of Karacostas (1988), using ISC data. We are confident in the depth of these events; we conducted additional tests to ensure that there was no systematic bias, with *P*-wave velocities in the crust ranging from 5.6 to 6.0 km s^{-1} and V_P/V_S ratios ranging from 1.70 to 1.77. Furthermore, some of these events are located with 22 *P* and 22 *S* arrival times, and with the azimuthal gap smaller than 90°. It is usually assumed that the depth distribution of earthquakes is related to the brittle deformation of the crust (e.g. Sibson 1984), or in the upper mantle (Chen & Molnar 1983). The seismically active lower crust beneath the western Peloponnese could

Table 2. (*continued*)

Nb	Date & Time	Lat °N	Long °E	Z km	Mag	Plan1		Plan2		P Axis		T Axis	
						As	Pl	As	Pl	As	Pl	As	Pl
726	860628 12:51	37.38	21.75	9.5	3.2	170	10	262	89	162	44	1	43
738	860628 23:48	38.14	21.64	22.7	3.4	225	90	315	90	269	0	180	0
739	860628 23:52	38.16	21.64	18.7	3.6	60	50	300	59	264	54	1	5
744	860629 5:52	37.70	22.02	17.2	2.3	330	50	150	39	60	5	239	85
756	860629 19:28	37.62	21.98	23.8	1.7	20	60	280	73	236	33	332	8
771	860630 8: 3	37.71	21.80	16.3	3.7	270	30	90	59	0	75	180	14
773	860630 9:57	37.72	21.81	15.6	3.6	230	70	120	46	95	46	349	14
806	860702 11:15	37.17	21.70	16.2	1.9	225	45	70	47	51	77	147	1
813	860702 20: 0	37.16	21.70	18.1	1.9	270	50	70	41	238	79	350	4
823	860704 14: 6	38.11	21.99	24.6	3.5	280	60	20	73	243	33	147	8
847	860707 17:14	38.27	21.79	12.8	2.4	240	90	180	0	150	45	330	45
888	860710 3:57	38.34	22.00	9.3	2.8	220	40	80	57	39	67	152	9
890	860710 6:30	37.79	21.12	8.6	3.4	190	10	10	80	99	35	279	55
893	860710 7:34	37.79	21.09	17.2	3.3	190	20	10	70	99	25	279	65
895	860710 8:24	37.77	21.13	10.1	3.0	330	30	120	63	1	68	220	17
899	860710 18:14	38.43	21.94	24.3	2.9	130	60	220	90	350	20	89	20
917	860711 13:32	37.51	21.88	20.7	1.7	230	60	120	59	85	45	354	0
935	860712 4:39	37.08	22.04	13.5	2.0	20	70	255	32	255	57	129	20
956	860713 1:57	37.40	22.01	15.8	2.0	290	60	170	49	146	54	47	6
968	860713 18:16	37.56	21.71	11.1	2.5	190	20	10	70	99	25	279	65
972	860713 21:22	38.42	21.79	18.7	2.5	210	70	110	64	71	33	339	3
994	860714 17:15	38.08	22.04	14.7	3.2	210	40	30	49	300	85	119	5
999	860714 21: 5	37.99	21.53	23.5	2.1	220	40	40	49	309	85	129	5
1000	860714 22:54	38.06	22.07	11.2	1.8	30	70	130	64	348	33	80	3
1001	860714 23:30	37.75	22.10	11.7	2.6	350	70	240	46	215	46	109	14
1005	860715 6:34	37.83	21.81	17.4	2.0	210	20	330	79	219	52	74	32
1013	860715 11:12	38.36	22.21	22.8	2.9	210	70	310	64	260	3	168	33
1026	860715 23: 6	37.83	21.84	9.7	2.0	140	20	232	89	122	42	340	40
1028	860715 23:42	37.70	22.01	16.8	1.9	200	80	290	90	64	7	155	7
1035	860716 2:55	36.04	23.77	21.4	4.0	195	50	40	42	42	76	296	3
1052	860716 20:28	37.70	21.63	24.0	1.8	180	70	0	19	270	25	90	65
1066	860717 15:27	37.82	21.47	23.9	2.6	350	80	250	45	220	38	112	21
81	860609 21:50	37.10	21.64	15.5	1.4	150	80	50	45	272	21	20	38
256	860614 17:50	36.03	21.97	.3	4.7	55	70	160	54	12	40	110	9
536	860622 8: 0	38.56	21.70	13.4	4.1	262	75	170	82	125	15	216	5
539	860622 9:21	38.56	21.68	16.3	3.7	270	80	170	45	140	38	32	21
543	860622 10:55	38.57	21.70	7.8	3.1	250	40	55	50	151	5	278	80
762	860629 22:37	36.87	21.44	26.2	3.1	150	15	15	79	297	54	96	33
805	860702 9:58	37.15	21.68	23.1	2.0	225	40	65	51	25	78	146	5
853	860707 22: 8	36.99	21.72	24.9	2.7	145	15	0	77	280	56	82	32
906	860711 1:51	37.17	21.81	13.0	1.9	105	60	330	39	328	64	213	11
934	860712 3:27	37.16	21.82	12.8	1.8	40	40	220	49	129	85	310	5
973	860713 21:58	37.11	21.82	14.0	2.0	160	28	0	63	289	70	83	17
1035	860716 2:55	36.04	23.77	21.4	4.0	195	50	40	42	42	76	296	3

For the solutions listed at the end (#81 to 1035) we relaxed some of the criteria.

reflect a higher degree of fracturing of the crust towards the western Peloponnese, as proposed by Leydecker, Berckhemer & Delibassis (1978), but possibly also a deepening of the geotherm which limits brittle and plastic deformation or an increase in the strain rate towards the west.

Fault plane solutions

We plotted the fault plane solutions on 2 maps, one for earthquakes deeper than 11 km, the other for earthquakes shallower than 11 km. We separated them because it appeared that the shallower events do not show any clear consistent pattern (except for the focal mechanisms located around the Gulf of Corinth), while fault plane solutions deeper than 11 km seemed to show some consistent spatial patterns.

The earthquakes shallower than 11 km (Fig. 7a), do not show a clearly consistent pattern in the type of mechanisms. We observe thrust faulting (#573 and #9), a few with strike-slip motion (#380 and 358) but also many normal faulting earthquakes, located in the western Peloponnese (#895) and around the Rio strait. We also observe some mechanisms with a sub-vertical plane and a sub-horizontal plane.

The earthquakes deeper than 11 km (Fig. 7b) show a similar pattern of shallow dipping plane and vertical plane striking NE–SW (#322, 890, 893, 431) but also E–W (#677, 119, 173). A quick look at the other mechanisms might give us the idea of chaos, because we observe reverse, strike-slip, and normal faulting.

A more careful look reveals a simpler pattern. The reverse faulting is mainly observed in the Gulf of Kephallinia and NW Peloponnese. The strike-slip faulting is seen around the Rio, in the northern Peloponnese and in central Peloponnese. All these strike-slip mechanisms are located between reverse faulting and normal faulting and generally show P-axes trending E–W and T-axes trending N–S. The normal faulting is observed in the Rio and northern Peloponnese, with T-axes trending mostly N–S, but also in the central and southern Peloponnese, with

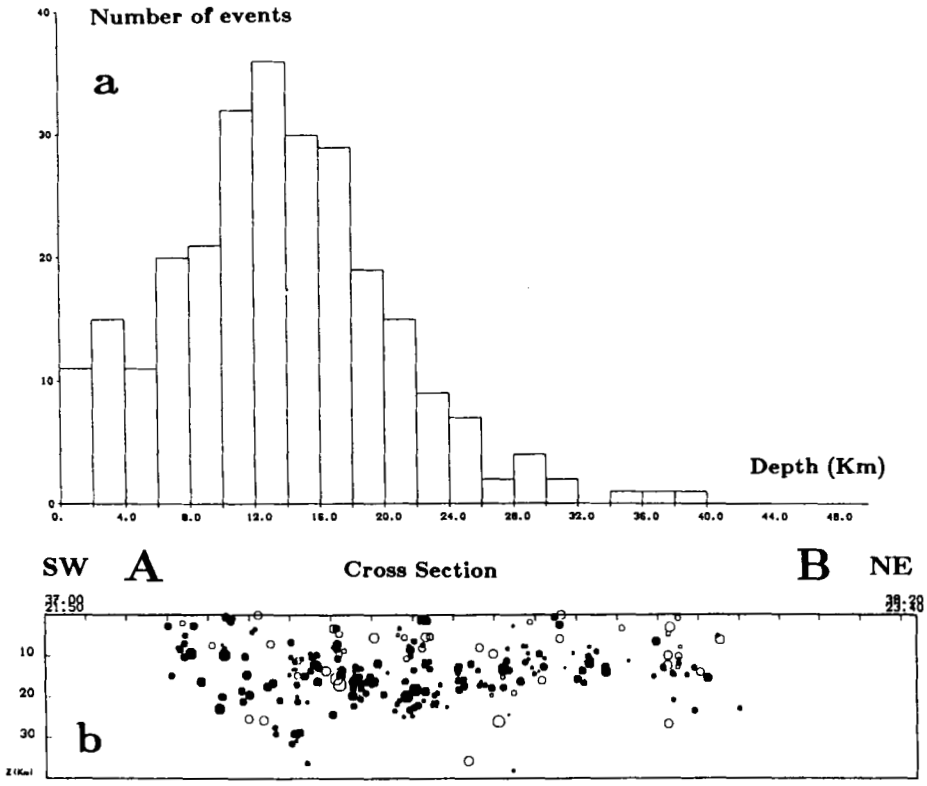

Figure 5. (a) Histogram of the depth of the earthquakes in the Peloponnese. (b) Cross-section of the crust beneath the Peloponnese (location in Fig. 4). The earthquakes are not only located within the upper crust and the depth of the foci increases towards the west.

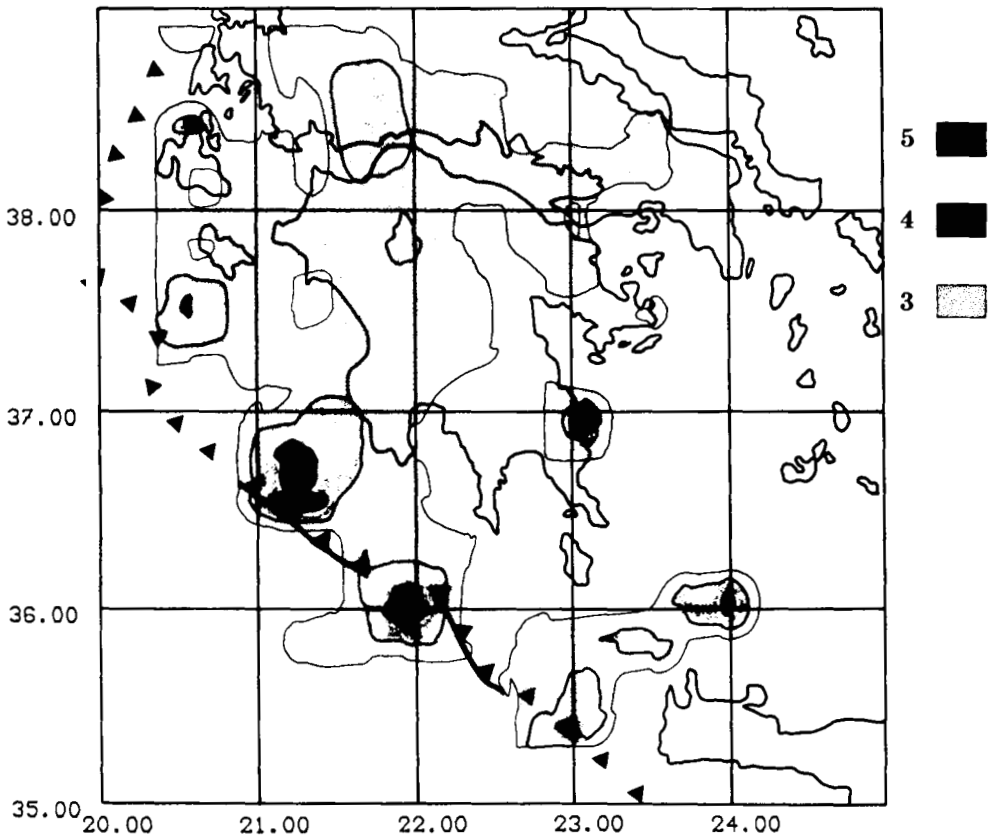

Figure 6. Map of the energy released during the experiment. The contour lines are the logarithm of the energy. The highest level is seen along the Hellenic trench with a maximum around the Matapan Mount, and within the Kythira strait.

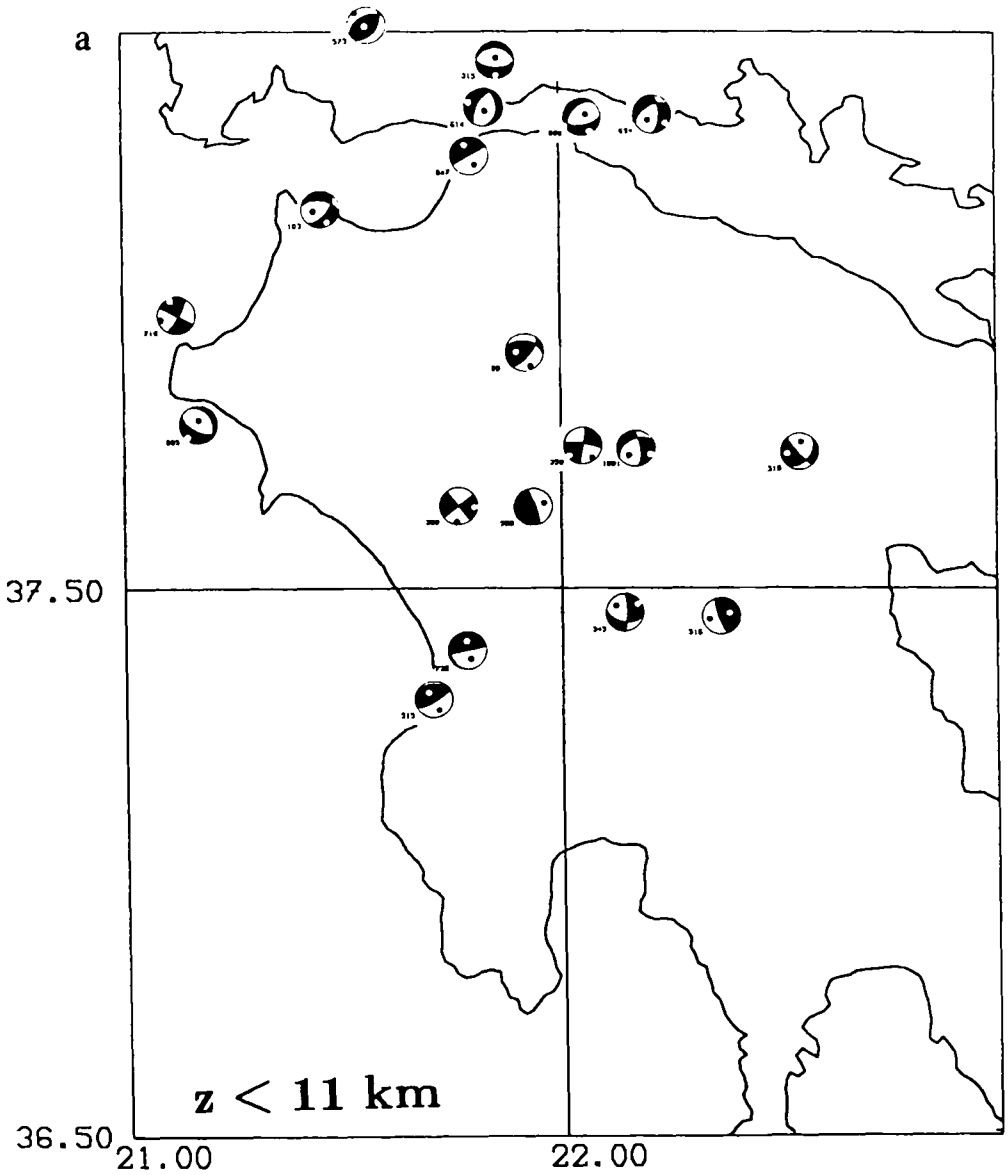

Figure 7. Map of the fault plane solutions. Lower hemisphere projection with compressive quadrants shaded. (a) Earthquakes shallower than 11 km, which do not show a clear pattern except around the Gulf of Corinth. (b) Earthquakes deeper than 11 km show thrust faulting in the western Peloponnese and normal faulting in the Gulf of Corinth, the central and southern Peloponnese.

T-axes trending NW–SE. So there is a regionalization of the faulting type, and also some continuity in the direction of *P*- and *T*-axes over most of the area.

Now we will comment in greater detail on some specific areas, where clusters are seen, and where we computed more focal mechanisms, relaxing some of the quality control.

The Ionian Sea

The earthquakes located along the Hellenic arc (Figs 3 and 4), within the Ionian Sea, are outside our network (we installed one station over the island of Strophades). Therefore the accuracy of the location could be questionable. Because most of the events were recorded by more than 15 stations, using both *Pg* and *Pn*, and because we conducted many tests for those events, we are relatively confident in, at least, the epicentres. Note that three clusters along the Hellenic trench are located in places where we observe a change in the direction of the trench as shown in Fig. 3.

The first (37.5°N, 20.5°E) is located south of Zakinthos, at the Zakinthos Trench, a basin as deep as 4000 m (Le Quellec *et al.* 1980), which could be related to the Hellenic trench. It is not well defined and includes about 20 events of magnitude ranging up to 4.2.

The second cluster is located around 36.7°N and 21.3°E, just north of the North Matapan trench. This was the most energetic area during our experiment (Fig. 6), and we recorded about 70 events of magnitude up to 4.7. This cluster shows a pattern trending NE–SW over 50 km, and could appear as an important fault, striking approximately NE–SW. This is approximately the direction of the Aegean–African relative motion in this part of the Hellenic

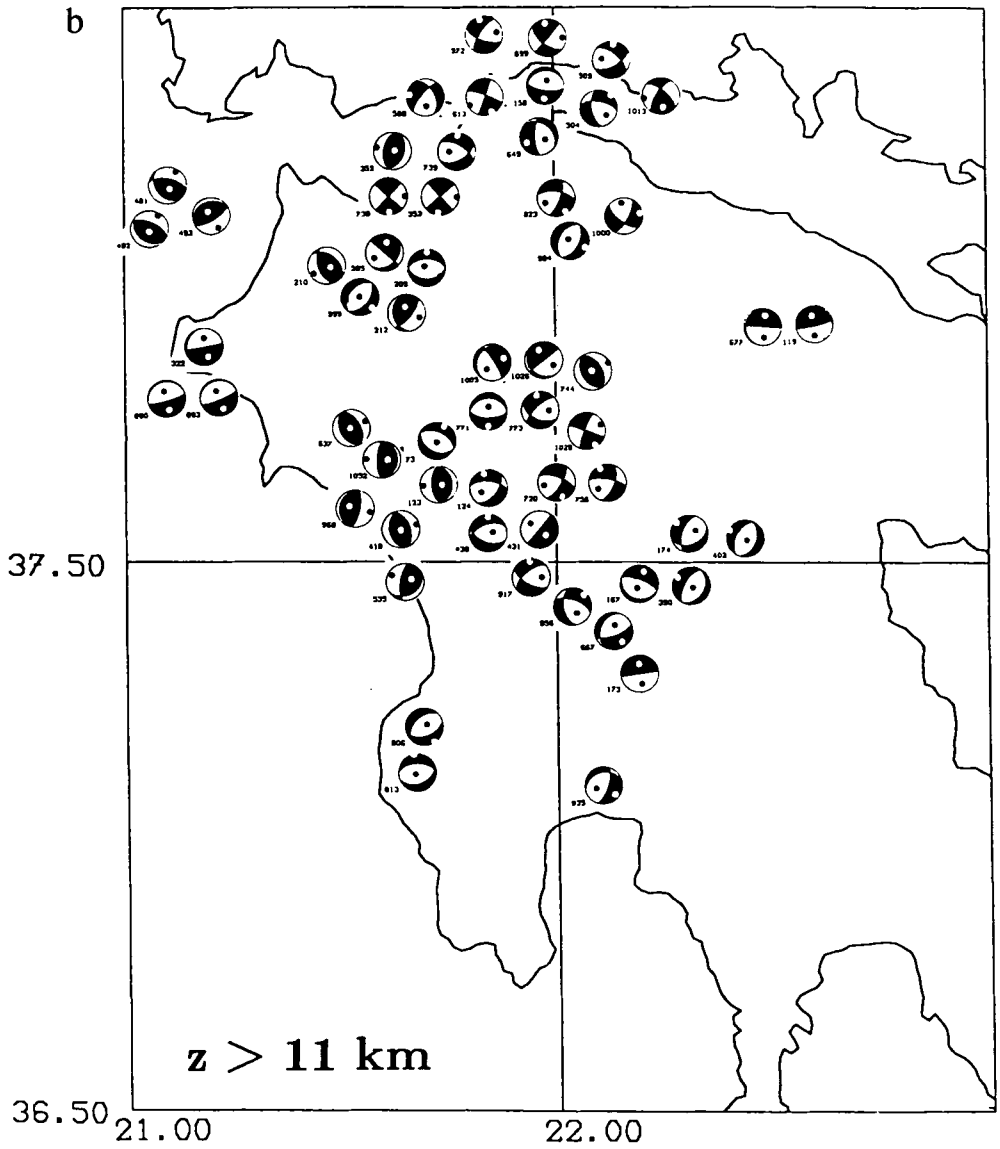

Figure 7. (*continued*)

arc (Angelier *et al.* 1982). Because most of the events were located using both *P*- and *S*-waves, we are quite confident in the epicentral distance to the network, and therefore we are confident in the shape and orientation of the seismicity. For this cluster, we could not compute individual fault plane solutions. Using polarities for four events, we found them to be inconsistent with any strike–slip mechanism. This NE–SW feature does not correspond to any bathymetric feature with the same trend. Therefore we doubt whether it can be related to any important strike–slip fault as suggested by the linear belt of earthquakes. This place is located north of the North Matapan trench (Le Quellec *et al.* 1980), which is considered as the place where the African–Aegean convergence changes from a subduction of oceanic lithosphere (in the south-east) to a collision between continental blocks (in the north-west), according to tectonic observations (Lyberis & Lallemant 1985; Le Pichon & Angelier 1979; Mercier *et al.* 1987). Therefore this cluster is found in a place where an important change in the mechanism of the convergence is likely to occur.

The third cluster is located south of the Peloponnese (36°N, 22°E). This is the location of the Matapan Mount (Fig. 8), a topographic high located between the North and South Matapan trench and which is thought to be a compressive structure due to the crushing of the sediments on the continental shelf (Le Quellec & Mascle 1979). The cluster is very well defined by about 30 events of magnitude up to 4.7. We computed one focal mechanism (#256), which is not very well constrained because the event occurred far outside of the network. This mechanism is consistent with normal faulting, with an important component of sinistral strike–slip motion, and with the *T*-axis trending ESE–WNW. This sinistral motion is contrary to the dextral strike–slip fault inferred by Le Quellec *et al.* (1980), south of the Matapan Mount, from the bathymetry.

The Kythira Strait

The Kythira Strait is located between the Peloponnese and Crete (Fig. 8), south of the South Matapan trench. This area is located at the southern part of the South Matapan trench;

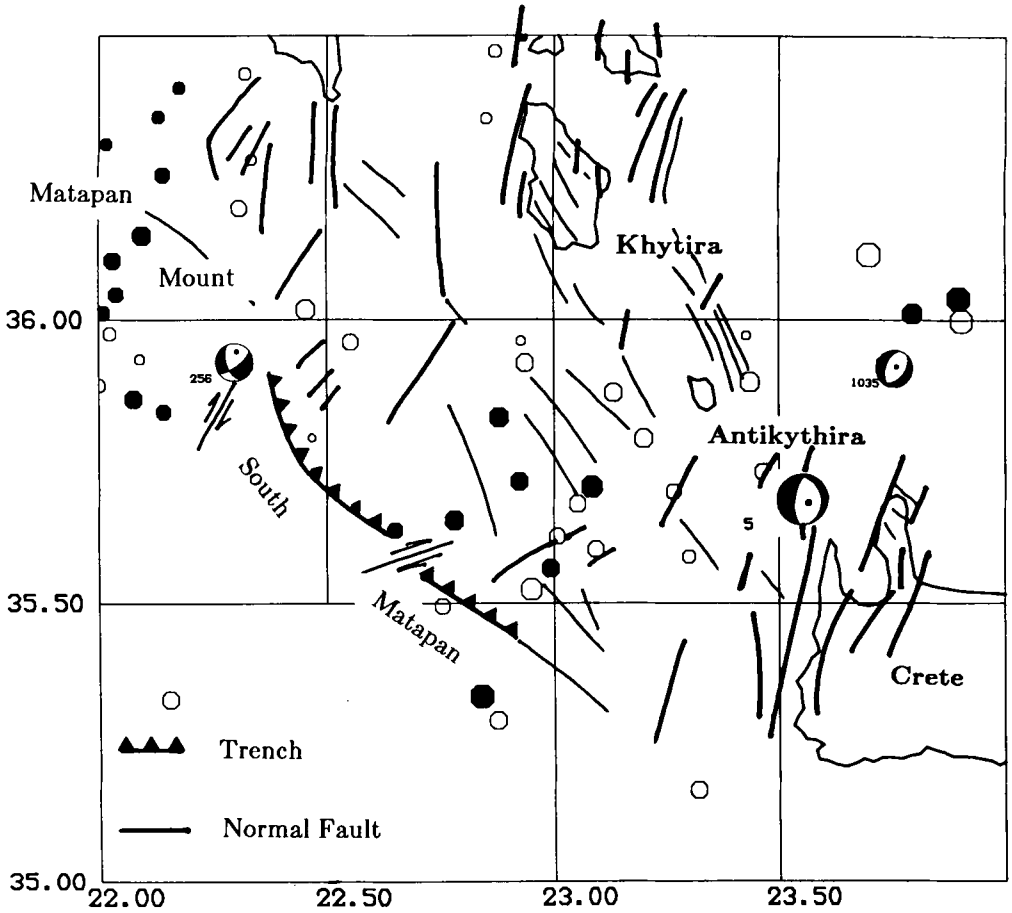

Figure 8. Seismicity map of the Kythira strait. The main tectonic features are from Lyberis *et al.* (1982) and Le Quellec *et al.* (1980). All the earthquakes are represented; the black symbols represent earthquakes which are located with accuracy better than 10 km. Fault plane solution #5 is from Lyon-Caen *et al.* (1988).

the tectonics is rather complex, showing two families of normal faults trending N–S and NW–SE, and probably due to the southern motion of Crete (Lyberis *et al.* 1982). Historical seismicity shows a gap for strong earthquakes during the last 2 centuries in this area (Ambraseys 1981; Wyss & Baer 1981; Papazachos & Comninakis 1982). Instrumentally located shallow seismicity, for the period 1917 to now, is also lower than elsewhere along the Hellenic arc (Makropoulos & Burton 1981; Comninakis & Papazachos 1986), as it is for intermediate depth events (Martin 1988). We had stations on Kythira and Antikythira and were able to locate quite accurately earthquakes in this area. During the 6 weeks of the experiment, we located about 15 earthquakes of magnitude up to 4.2, and these events show a pattern striking NE–SW. This is quite surprising in light of the active N–S normal faulting as inferred from the bathymetry and seismic reflection data (Lyberis *et al.* 1982). We computed one focal mechanism (#1035), which shows normal faulting with the *T*-axis trending NW–SE, and is consistent with the two mechanisms both of moderate earthquakes in this area in 1965 (McKenzie 1978; Lyon-Caen *et al.* 1988) and in Kalamata (Lyon-Caen *et al.* 1988; Papazachos *et al.* 1988).

Before going farther, it is worth noting that all these clusters are located at places where we observe a change in the bathymetry of the trench: the Zakinthos basin, the North Matapan trench, the Matapan Mount, and the South Matapan trench. All of these clusters show a NE–SW orientation, and could be associated with stress concentration in the places where the relative motion between Africa and Aegea is not uniform.

The Gulf of Kephallinia

The seismicity located around and west of the Ionian islands is well known, and an episode of intense seismic activity occurred in 1983 (Scordilis *et al.* 1985). We did not record many earthquakes during our experiment in this area, although we had stations on Kephallina, Zakinthos, Lefkada and Ithaki. On the other hand, we recorded a few earthquakes in the Gulf of Kephallinia, with magnitudes ranging up to 3.1, and which are very well clustered (Figs 3 and 4). This place has not been considered seismically active, and no earthquakes were recorded during a 2-month experiment in this area in 1979 (H. Haessler, personal communication, 1986). The depths of the well-located (better than 5 km) events range from 20 to 33 km. We computed three fault plane solutions (#481, 482, 483 in Fig. 7). These show reverse faulting, two with a *P*-axis trending NE, one trending NW. This pattern of reverse faulting is similar to the fault plane solutions computed in this area (McKenzie 1978; Jackson *et al.* 1981; Scordilis *et al.* 1985;

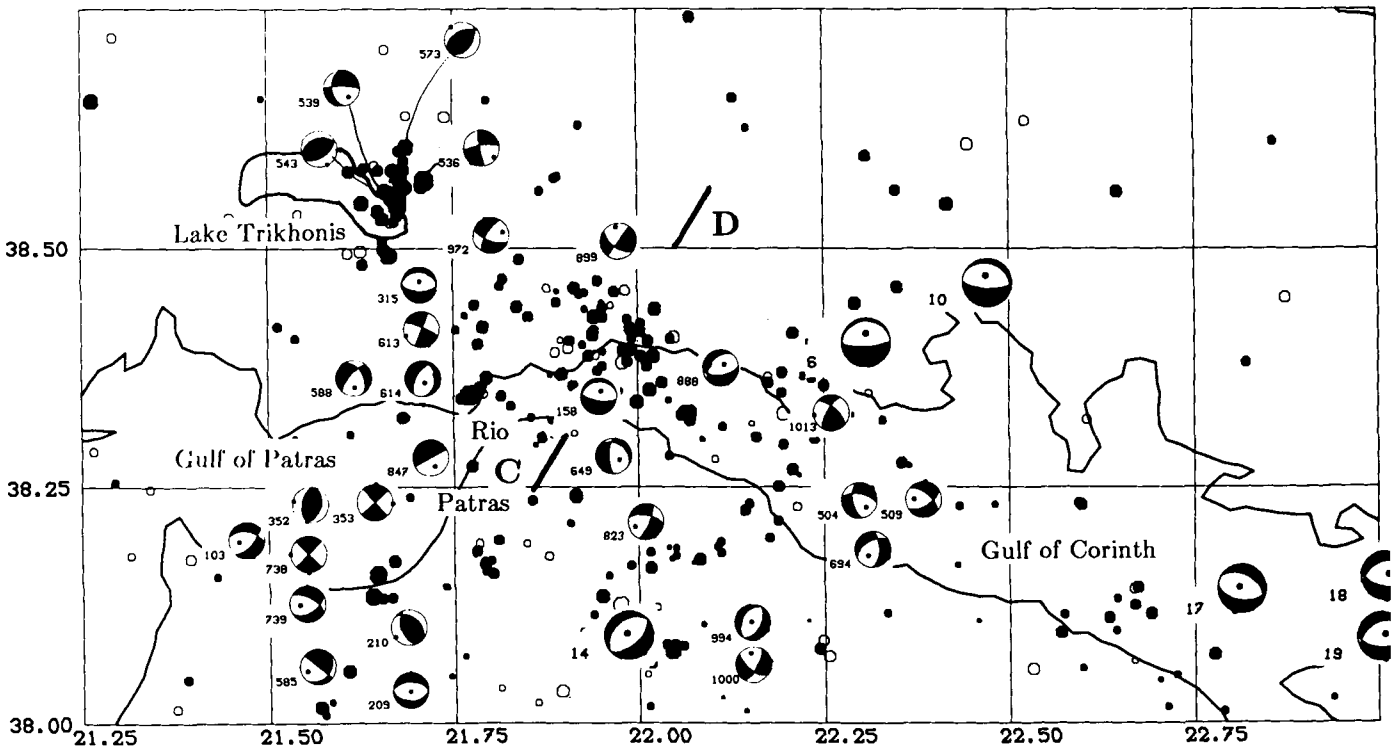

Figure 9. Seismicity map of the Gulf of Patras and the Gulf of Corinth. Notice the cluster located east of the lake Trikhonis, with reverse and strike faulting showing *P*-axes trending NW–SE. Notice also the cluster around the Rio and the location of the cross-section C–D. Fault plane solutions #6 and 10 are from McKenzie (1978), #17–19 are from Jackson *et al.* (1982).

Anderson & Jackson 1987). Bathymetric and seismic reflection profiles (Brooks & Ferentinos 1984) show that this area has been in NE–SW compression since early Pliocene time.

The Gulf of Patras and Gulf of Corinth

In this area, there are two important clusters of seismicity (Fig. 9).

The first, consisting of about 50 events of magnitude up to 4.0, strikes N–S, east of the Lake Trikhonis. This area was not known to be seismically active (Melis, Brooks & Pearce 1989). The depths of the well-located earthquakes range from 5 to 20 km. Because they are located outside of the seismological network, we used *Pn* polarities to compute fault plane solutions. Two mechanisms (#543, 573) show reverse faulting, with the *P*-axis trending NW–SE, and two others (#536, 539) show strike–slip motion with similar *P*-axes. The results are quite surprising, because the Lake Trikhonis is known to be located between two E–W normal faults (Doudsos, Kontopoulos & Frydas 1987; J. Jackson, 1987, personal communication) in the Plio-Quaternary time, (Brooks *et al.* 1988).

The second cluster is located around the Rio, between the Gulf of Patras and the Gulf of Corinth. This is known to be a very active seismic area (Papazachos & Comninakis 1971; Makropoulos & Burton 1981; Melis *et al.* 1988). During our experiment we recorded about 80 earthquakes of magnitude up to 3.0 in this area. A cross-section, striking NE, shows a deepening in the events, from 5 to 15 km, towards the NE (Fig. 10). This observation is consistent with the results of

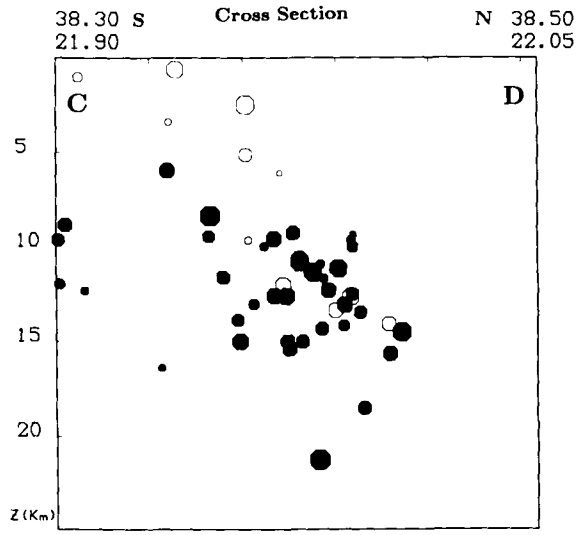

Figure 10. Cross-section of the Rio cluster showing the deepening of the earthquakes towards the NE.

Melis *et al.* (1989). We computed 16 focal mechanisms (Fig. 9); most of them show N–S normal faulting which is consistent with the mechanisms computed for larger events in this area (McKenzie 1978; Jackson *et al.* 1982), or surface faulting of historical events (Papazachos *et al.* 1984); a few (#613, 899, 1013) show strike–slip faulting. Two earthquakes located in this area, at 53 and 71 km deep, also show N–S extension with a strike–slip component (Hatzfeld *et al.* 1989). The tectonics of this area are complex, located

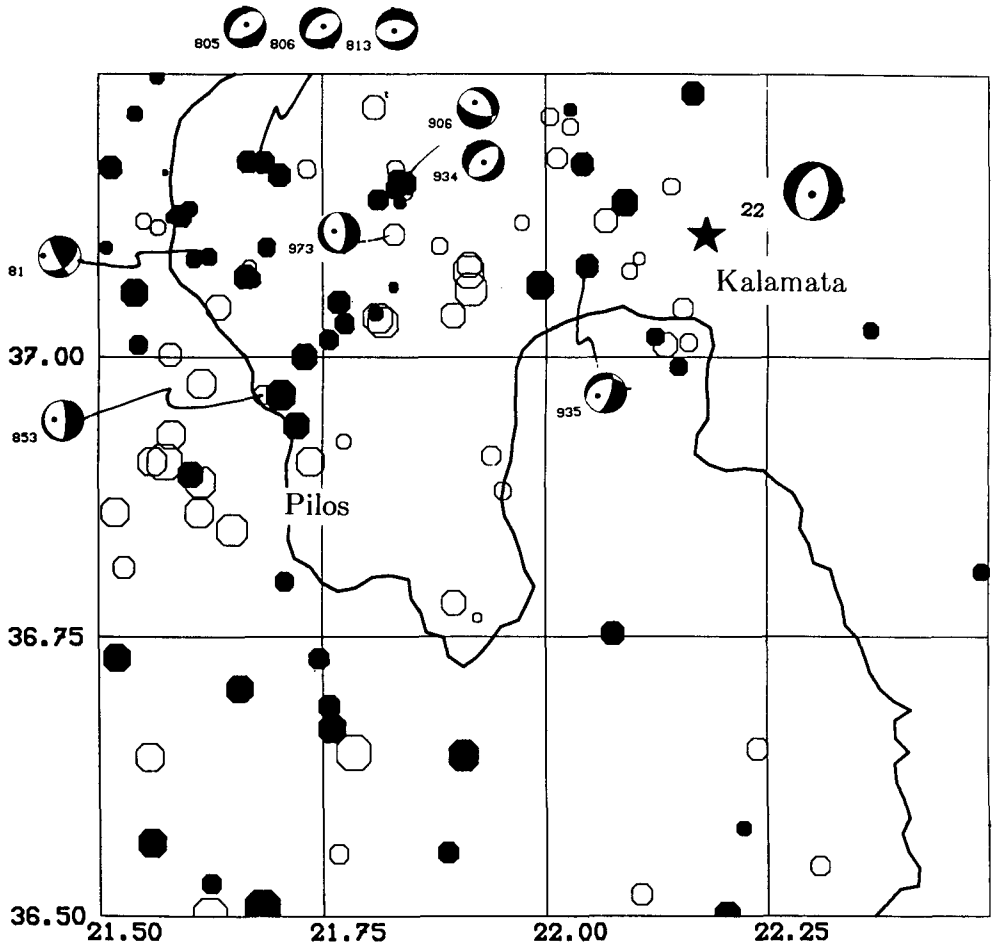

Figure 11. Seismicity map of the Kalamata region. The star is the epicentre of the earthquake of magnitude 5.8 which occurred on 1986 September 13. Fault plane solution #22 is from Lyon-Caen *et al.* (1988).

at the intersection of two graben systems (Doudsos, Kontopoulos & Ferentinos 1985; Brooks & Ferentinos 1984; Ferentinos, Brooks & Doudsos 1985). Brooks *et al.* (1988) interpret the pattern of neotectonics and seismicity as a transfer fault system between the Gulf of Corinth and the Lake Trikhonis. Our observations do not show any strike–slip motion west of the lake Trikhonis, but could be consistent with strike–slip east of the lake.

Kalamata

Eight weeks after our experiment, a destructive earthquake of magnitude $Ms = 5.8$ occurred in Kalamata (Lyon-Caen *et al.* 1988; Papazachos *et al.* 1988). Because our network included a station in Kalamata, we tried to look for any peculiar pattern of seismicity. We checked carefully the Kalamata records and did not find any abnormal pattern in the level of the seismicity. Also, the seismicity map (Fig. 11) does not show any specific cluster. One fault plane solution (#935) shows NW–SE normal faulting which is in agreement with the focal mechanism of Kalamata. Focal mechanisms were also computed west of Kalamata. Most of them show normal faulting, the T-axes trending NW–SE (#805, 806, 813, 934, 935), or NE–SW (#906).

DISCUSSION

The fault plane solutions

Focal mechanisms are representative of the displacement and strain fields and (with some hypotheses) of the stress field. For strong earthquakes ($mb > 5.5$) we can consider the crust as a homogenous medium compared to the fault length, and the slip vector is the important parameter. For smaller magnitudes, however, local heterogeneities (as pre-existing faults) could introduce weakness zones and the relation between the stress tensor and the P-, B- and T-axes is not obvious (McKenzie 1969; Célérier 1988). Within a pre-fractured medium, as is often the continental crust, for such small fault lengths, it is not practical to discuss every single fault plane solution to get a fault plane and a slip vector, but we have to look for consistency in the pattern deduced from the P- and T-axes. In the following part we will attempt to deduce a strain pattern for the western Hellenic arc from the focal mechanisms.

As mentioned before, we observe four different families of focal mechanisms.

(a) Shallow dipping nodal planes are observed for earthquakes over all of the Peloponnese. For these we observe several orientations of the steep planes: most of

them have the vertical plane trending E–W, usually with the northern hemisphere moving down (#119, 173, 515, 677, 726, 847, 1026), but also up (#322, 890, 893) around Kyllini. We observe others with the vertical plane trending NNW–SSE (#516, 560, 585, 1005) and one with the vertical plane trending NE–SW (#431), which is the deepest event of this family.

There is no obvious explanation for these shallow dipping mechanisms. Neither the *P*-axes nor the *T*-axes show any consistent pattern, and there is no geographical regionalization. We can only observe that most of these earthquakes occurred between 8 and 18 km. The only consistent pattern is the flat nodal plane, and one possible explanation for such type of mechanism over a wide area could be a surface of decoupling between the upper and the lower crusts.

(b) Reverse faulting is mainly observed in the westernmost part of the studied area around Kefallinia, as it is also in neotectonic observations (Sorel 1976; Mercier *et al.* 1979; Lyberis & Lallemant 1985) or from seismic reflection data (Brooks & Ferentinos 1984). It is also observed in the western Peloponnese, and around the Trikhonis lake, where neotectonic studies suggest N–S extension (Mercier *et al.* 1987). Only one thrust is observed in the central Peloponnese (#744). The mean azimuth of the *P*-axes for two focal mechanisms in the Gulf of Keffalinia (#481, 482) is N43°E, similar to the value of N55°E computed using stronger earthquakes (Anderson & Jackson 1987). It is N95°E for the earthquakes located further east in the Peloponnese (#352, 212, 1052, 968, 418, 535, 744). Thus we observe a slight and progressive rotation of the *P*-axes of earthquakes from east to west, which is consistent with the two mechanisms located in the western Peloponnese (#210 and 637). The foci are located between 10 and 29 km deep, with a maximum around 22 km.

(c) Normal faulting is observed from the Gulf of Corinth to Kythira, with the *T*-axes trending in various directions. Around the Gulf of Corinth and northern Peloponnese, the *T*-axes trend mostly N–S, as they do for stronger earthquakes (McKenzie 1972, 1978; Jackson *et al.* 1982). This direction of extension is also consistent with neotectonic observations (Sébrier 1977; Angelier 1979; Mercier *et al.* 1979) and faulting of historical events (Papazachos *et al.* 1984).

Normal faulting is also seen in Central Peloponnese, but the trend of the *T*-axes changes from N–S to NW–SE. This NW–SE orientation is seen near Pilos and Kalamata (Fig. 11), but also around Antikythira (Fig. 8), and also was observed for the available mechanisms computed from WWSSN data (McKenzie 1978; Lyon-Caen *et al.* 1988; Papazachos *et al.* 1988).

Neotectonic observations (Sébrier 1977; Angelier 1979; Mercier *et al.* 1979; Angelier *et al.* 1982; Lyberis, Lallemant & Thiebault 1983) also show a rotation in the direction of extension, trending N–S around Olympia but NW–SE south of 37.5°N, but the change in strain pattern that they inferred is more abrupt than what we observe.

The depth of the events showing normal faulting are mostly located between 4 and 22 km, with a strong maximum around 12 km, and another around 18 km. It is worth noting that all the normal faulting events shallower than 18 km are located in the western Peloponnese while the deepest events are located in the centre.

(d) Strike–slip faulting is observed around the lake Trikhonis, where the *P*-axes trend NW–SE (consistent with two reverse mechanisms of this area, #543 and 573). Strike–slip faulting is also observed around the Gulf of Corinth, where the *P*-axes trend E–W and the *T*-axes N–S, which is also consistent with the normal and reverse faulting in this area. We do not observe strike–slip faulting in the area south of where reverse faulting is observed.

One strike–slip fault, with the same orientation for the *T*- and *P*-axes, was computed using WWSSN data (McKenzie 1972; Lyon-Caen *et al.* 1988), for an earthquake located in the western Peloponnese (Fig. 12).

As far as we know, there is no observation of strike–slip faulting from neotectonic studies. Nor do we observe a pattern of seismicity which could be related to such faulting. Therefore the observed strike–slip mechanisms probably represent a transition between regions of normal and thrust faulting.

Strike–slip faulting shows two families of depths: one around 10 km, and another around 18 km. As for shallow dipping mechanisms, there is no regionalization with depth.

The style of deformation

A map of the style of deformation (Fig. 12) allows a better visualization of the different types of deformation. We use the data from our study as well as reliable fault plane solutions deduced from WWSSN data (McKenzie 1972, 1978; Jackson *et al.* 1982; Lyon-Caen *et al.* 1988). We observe reverse faulting in the western Peloponnese but only north of 37.5°N. Published focal mechanisms show that reverse faulting is also observed all along the Hellenic trench. In the internal part of the arc, we observe normal faulting, from the Gulf of Corinth to Crete. The transition between reverse faulting and normal faulting is rather sharp, but with some overlap of the two families, especially in the northwest. In the same area where the normal faulting exists, we also observe strike–slip mechanisms; these mechanisms characterize earthquakes only north of 37.5°N, where reverse faulting is observed.

The strain pattern deduced from the fault plane solutions is different from that deduced from neotectonic observations (Angelier *et al.* 1982; Mercier *et al.* 1987). Both observations show the compression in the western part of the Hellenic arc, the N–S extension around the Gulf of Corinth and E–W extension in the southern Peloponnese. But our observations differ in that we find compression in the western Peloponnese, where neotectonic studies show E–W extension.

The pattern of horizontal strain

The next step will be to map the trajectories of the horizontal principal strain, assuming that the *P*-axes represent principal axes of shortening, and the *T*-axes principal axes of extension.

Figure 13 shows the strain field deduced from our data and other WWSSN fault plane solutions. The pattern of strain trajectories is somewhat different from both that proposed by Le Pichon *et al.* (1982), deduced from sea-beam and neotectonic observations, and that proposed

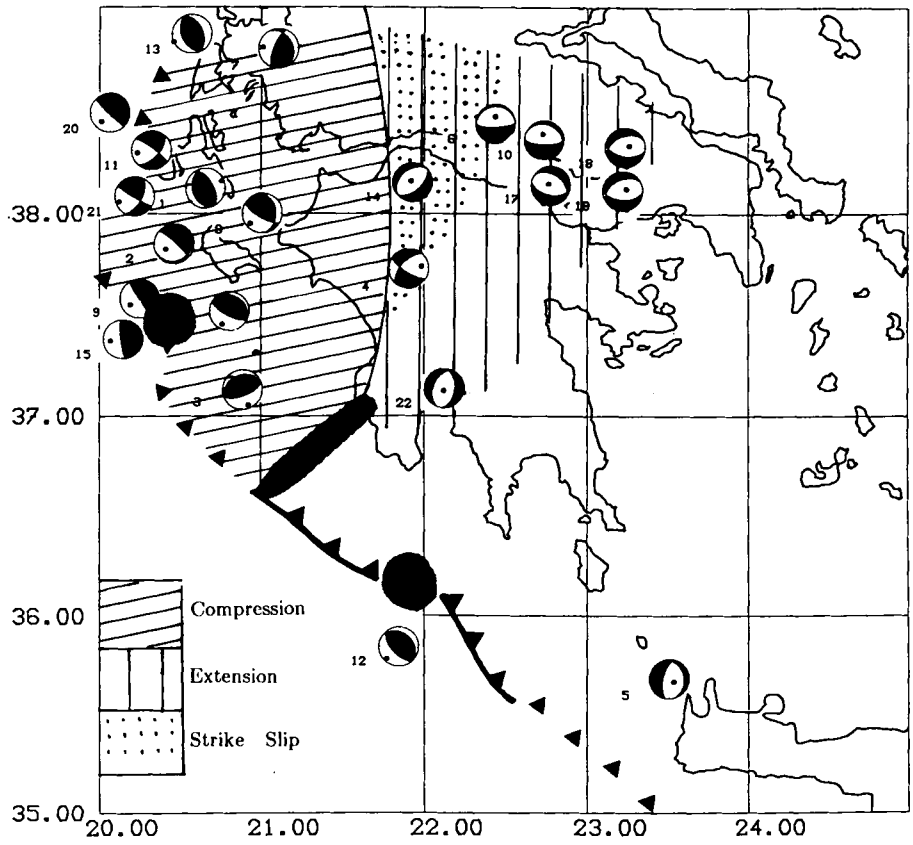

Figure 12. Map of the style of deformation observed in the western Hellenic arc. Compression is seen from the trench to western Peloponnese. Fault plane solutions are taken from the literature and referenced in Table 3. The transition between compression and extension is sharp, and in some place we observe strike–slip mechanisms within the extensive stress field. The three shaded areas are the three dense clusters of seismicity. The transition between compression and extension occurs where the Hellenic trench is less defined.

Table 3. Parameters of the fault plane solutions (WWSSN).

Nb	Date & Time	Lat °N	Long °E	Z km	Mag	Plan1		Plan2		P Axis		T Axis		Ref
						As	Pl	As	Pl	As	Pl	As	Pl	
1	530812 09:23	38.11	20.72	.0	7.2	163	34	330	56	65	11	216	77	McK
2	591115 17:08	37.80	20.56	.0	6.6	66	16	310	82	235	50	27	36	McK
3	631216 13:47	37.10	20.90	15.0	5.6	64	64	244	25	154	19	333	71	AJ
4	650405 03:12	37.70	21.80	34.0	5.7	226	58	125	73	81	35	178	9	McK
5	650427 14:09	35.70	23.50	13.0	5.7	191	65	346	27	122	68	272	19	LC
6	650706 03:18	38.40	22.40	20.0	5.9	265	14	87	76	357	58	176	31	McK
7	661029 02:39	38.81	21.10	20.0	5.7	204	70	334	29	277	21	145	58	AJ
8	680328 07:39	37.90	20.90	6.0	5.4	120	71	357	32	229	21	355	55	AJ
9	690708 08:09	37.56	20.28	33.0	5.4	145	88	325	1	234	43	54	47	AJ
10	700408 13:50	38.43	22.66	17.0	5.8	90	70	294	21	345	63	186	24	McK
11	720917 14:07	38.28	20.34	33.0	5.6	306	80	42	59	259	28	357	13	AJ
12	730105 05:49	35.81	21.84	33.0	5.3	136	60	307	30	222	14	58	74	McK
13	731104 15:52	38.90	20.44	8.0	5.8	336	44	156	45	246	1	65	89	AJ
14	750404 05:16	38.09	21.98	53.0	5.4	46	54	226	35	315	81	136	9	McK
15	760511 16:59	37.56	20.35	33.0	5.8	172	80	352	9	262	35	82	55	AJ
16	760612 00:59	37.54	20.55	8.0	5.5	115	70	295	19	204	25	25	65	AJ
17	810224 20:53	38.10	22.84	10.0	5.9	300	42	99	49	309	78	198	4	J
18	810225 02:35	38.14	23.05	8.0	5.5	247	42	100	52	67	72	175	5	J
19	810304 21:58	38.18	23.17	8.0	5.9	90	52	240	42	58	73	166	5	J
20	830117 12:41	38.30	20.23	14.0	6.1	135	83	315	6	224	38	45	52	AJ
21	830323 23:51	38.29	20.26	19.0	5.8	27	59	120	85	249	17	348	25	AJ
22	860913 17:24	37.08	22.15	11.0	5.5	201	45	3	46	196	80	101	0	LC

McK=McKenzie (1978)
AJ=Anderson & Jackson (1987)
LC=Lyon-Caen et al. (1988)
J=Jackson et al. (1981)

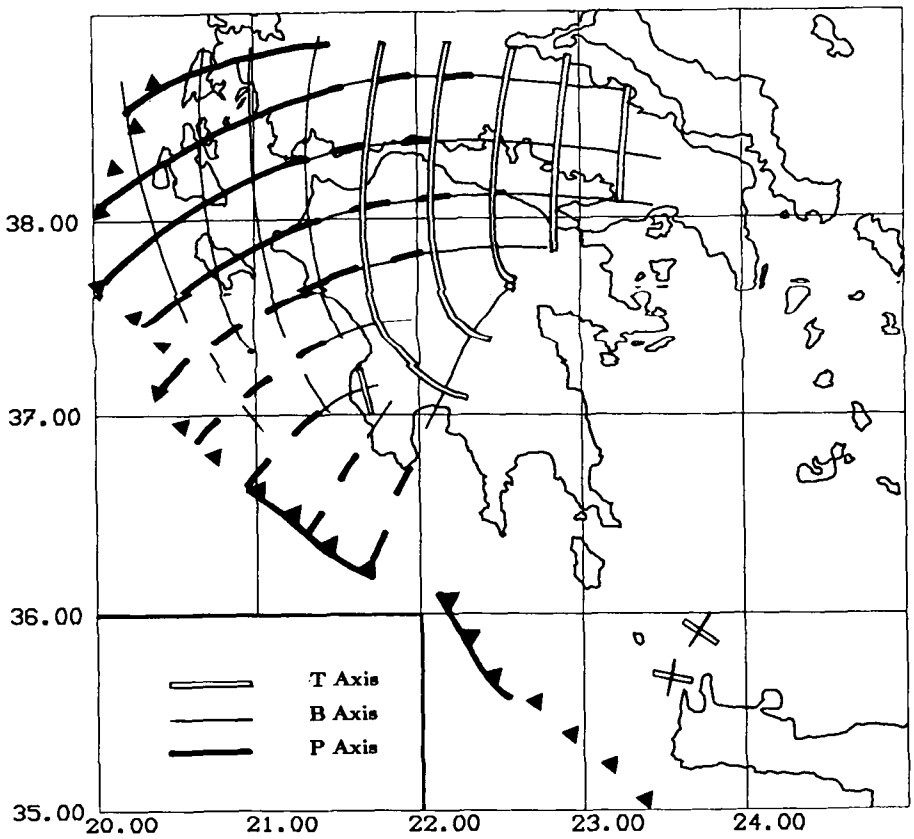

Figure 13. Map of the stress trajectories deduced from our study and other focal mechanisms. Ticks are interpolation of the observations. The compressive stress, rotating from NE–SW along the trench to E–W in the Peloponnese is likely to be due to the locking of the overthrusting of the Aegean plate over Apulia. Normal faulting is seen in a more internal position. A rotation of the *T*-axes is observed where the trench is less marked in the bathymetry.

by Mercier *et al.* (1987), using neotectonic observations and fault plane solutions.

Along the western Hellenic arc the compression is orientated NE–SW, from the Ionian islands to south of the Peloponnese. This direction is slightly different from that observed south of Crete (Taymaz 1989). Within the western Peloponnese, we observe E–W compression, implying a rotation of the axis of compression, from NE–SW on the coast to E–W inland. This E–W direction is also observed, in scattered areas, far from the trench. For instance, some strike-slip mechansims within the Gulf of Corinth show *P*-axes trending E–W; this is also the case in central Peloponnese. Similarly, the orientation of extension, which is N–S in the northern Peloponnese rotates to be E–W towards the southern Peloponnese and Crete. This rotation is seen north of the North Matapan trench, where the morphology of the Hellenic trench changes from a deep feature southward to a smooth topography northward (Le Quellec *et al.* 1979). This change in the topography is sometimes associated with a difference in the subduction mechanism, north and south of this point.

The transition from dominantly E–W compression to dominantly N–S extension occurs in a few tens of kilometres, and in this transition zone we observe strike-slip motion. Therefore, we think that the deviatoric stress is probably small, because the earthquakes are due to differential stress, and because stress cannot change very much over a short distance. If over a short distance reverse faulting gives way to normal faulting, the values of the extensile and the compressive stresses are similar. The strike-slip faulting represents the transition between the two stress fields.

However there are a few exceptions to this pattern, with pairs of focal mechanisms (normal and reverse) having the same *B*-axis, and therefore interchanging *P*- and *T*-axes (e.g. #212 and #999, #744 and #1005). For those pairs we have to imagine abrupt heterogeneities in the stress field which could be due to pre-existing faults as seen in the Mygdonian graben (Hatzfeld *et al.* 1986).

Implications of the strain pattern

Several maps of strain trajectories have been proposed for the Aegean arc. These maps come mainly from neotectonic observations, from fault plane solutions of the large earthquakes and from the bathymetry. Their geodynamical implications are quite different from one another.

As pointed out by Mercier (1981), Angelier *et al.* (1982), Lyberis & Lallemant (1985) and Mercier *et al.* (1987), extension is approximately N–S around the Gulf of Corinth, and E–W in the Southern Peloponnese and Crete, but the neotectonic observations are very scarce, and the model of

strain pattern will strongly depend on the way the observations are smoothed. The new observations coming from our data show a slight rotation of the maximum compression strain in the western Peloponnese and also show a progressive and important rotation of the extensile strain within the Peloponnese. This rotation is observed approximately in the area where we mapped a dense cluster in the seismicity; this cluster is located where a marked change in the morphology of the trench is also observed.

Assuming that the strain field is proportional to the deviatoric stress field, it is not possible to explain non-uniform stress pattern in a rigid lithospheric plates scheme; therefore, we will try to examine the different strain patterns and their geodynamical implications.

It seems clear that the Aegean 'plate' is thinning and extending over the African plate. This idea has been introduced for the Aegean crust by McKenzie (1978) and developed for the whole lithosphere by Le Pichon & Angelier (1979) with the addition of forces coming from the sinking slab which progressively retracts towards Africa. The Mediterranean Ridge is the front of the underthrusting of the African plate beneath Agea when the Hellenic trench is considered as a fore-arc basin. The slope of the subducted lithosphere is very shallow for about 250 km between the Mediterranean Ridge and the Hellenic trench (Le Pichon *et al.* 1982). It is dipping slightly more (about 10°), beneath the Peloponnese, from the trench to the Gulf of Argolia (Hatzfeld *et al.* 1989), and also beneath Crete (Martin 1988). It is difficult to imagine any other mechanism to explain this very shallow dipping slab over 400 km. The slope of the subducted slab is the response to the loading of the accretionary prism of sediments for the first portion (Le Pichon *et al.* 1982) and to the Aegean lithosphere for the last portion (Hatzfeld *et al.* 1989).

The change in the morphology of the Hellenic trench north of 36.5°N and 21.0°E reflects the difference in the type of the overthrusting. As proposed by Lyberis & Lallemant (1985), it seems probable that the convergence rate is smaller north of the Ionian islands. One cause would be the difficulty for the Aegean 'plate' to overthrust the Apulian plate, because of the buoyancy of a thick continental lithosphere. But palaeomagnetic measurements do not support the idea of an important discontinuity between southern Apulia and northwestern Greece (Tozzi *et al.* 1988).

Using tectonic observations, Angelier *et al.* (1982) suggest that the N–S extension observed in the northern Peloponnese rotates clockwise to be E–W in the southern Peloponnese and Crete. Their model associates the direction of extension of the Aegean lithosphere with the flow of the Aegean lithosphere. The locking of the Ionian branch behaves as an obstacle and modifies the flow in the southern Peloponnese (Lyberis & Lallemant 1985).

Mercier (1981) and Mercier *et al.* (1987) suggest that the orientation of extension rotates counterclockwise from the Gulf of Corinth to Crete. In their model the compression is perpendicular to the boundary, which is the Hellenic arc, and the extension is parallel and due to the variation of crustal thickness and the deep thermal structure.

In Lyon-Caen *et al.* (1988), the observed stress field in the Peloponnese and the Kythira strait is the superposition of the main Aegean N–S extension, observed from the northern to central Aegean, and a secondary E–W strain field due to the incoming African margin across the Hellenic subduction, observed only in the southern part.

As shown by experimental modelling (Merle 1989), spreading produces a complex pattern of finite deformation which does not follow the particle trajectory: in the centre the stretching is mostly radial and the elongation ratio can reach values up to 40, then going to the periphery it becomes concentric and finally the stretching is mostly tangential near the convex side of the nappe. Moreover the maximum strain is observed at the contact between the base and the nappe.

Therefore, assuming a spreading mechanism for Aegea, we should observe compression at the trench and longitudinal extension in an internal position; this is roughly what the fault plane solutions are showing in the area where the Helenic subduction is clear.

In the western Peloponnese, Aegea is not spreading freely towards the west because of Apulia. In order to estimate the effect of the collision of Aegea with Apulia we can consider it as an indenter for Aegea. England, Houseman & Sonder (1985) showed that the rigid indentation of a thin viscous sheet produces a field of deviatoric stress over an area whose width is of the order of its length. Moreover, Houseman & England (1986) show that the compression, which is perpendicular to the indenter at the boundary, rotates progressively when going away from the boundary. In our case this would produce a clockwise rotation of the *P*-axes from the Ionian islands inland.

Therefore, we suggest that the observed strain field in the western Hellenic arc is the result of the superposition of two stress fields (Fig. 14), keeping in mind that the boundary conditions are different and the effect non-linear. One is due to the buoyancy of the crust and hot upper mantle of Aegea, which is responsible for the radial compression observed along the arc and for the longitudinal extension observed in the Gulf of Corinth and in southern Peloponnese and Crete. The other due to the collision with a continental block, Apulia is a good candidate even the boundary is not clear (Tozzi *et al.* 1988), and superposes a compressive stress field which varies progressivly from NE–SW to E–W. In the area where the maximum compressive stress of one equals the maximum tensile stress of the other, we observe a switch from E–W compression to N–S extension, or strike–slip mechanisms. But small perturbations in the stress field (due to local conditions) could modify the resultant stress field and this is the reason why we observe, locally, *P*-axes trending E–W, far from the boundary.

CONCLUSION

Results from microearthquakes surveys are always suspicious in terms of understanding geodynamical processes. The energy released during such experiments is fairly small compared to that from earthquakes with a magnitude greater than 6.0, and the faults inherited from previous tectonics can make any interpretation difficult.

In order to overcome these difficulties a few precautions have to be taken into account. It is necessary to record enough earthquakes to smooth the local conditions, and see a possible pattern. They have to be recorded by many stations in order to bring more detailed information than

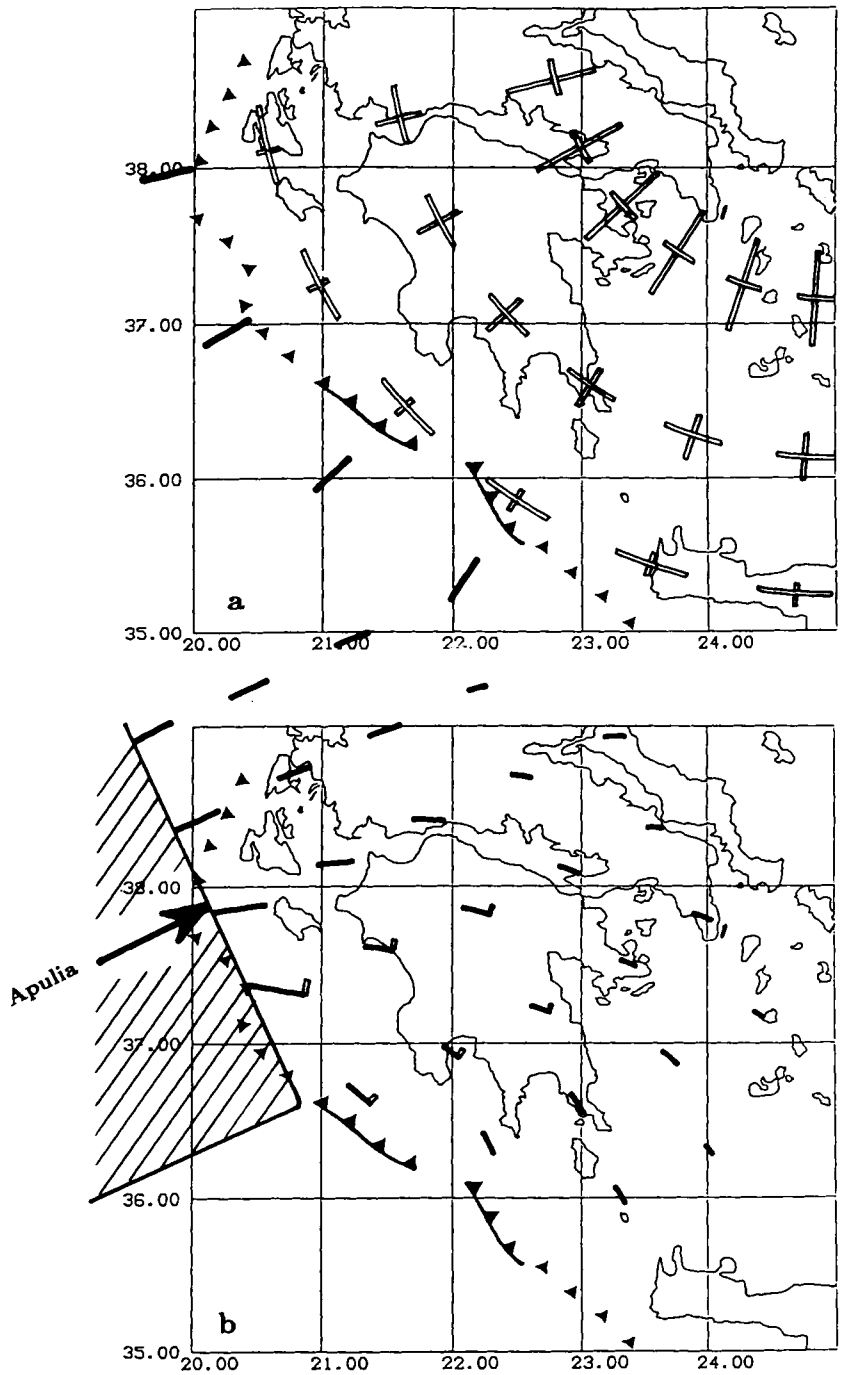

Figure 14. The observed stress trajectories is likely to be due to the superposition of two stress fields illustrated very crudely (boundary conditions are different and effects are non-linear) as follows. (a) A stress field due to the spreading of Aegea. This stress field is deduced from incremental deformation of gravity nappes observed in experimental modelling (Merle 1989). (b) A deviatoric stress field due to Apulia which behaves as an indenter for Aegea. The contour of Apulia is certainly oversimplified. This stress field is deduced from numerical experiments computed by Houseman & England (1986).

strong earthquakes. If these conditions are fulfilled, they allow a significant interpretation.

Installing a dense network of seismological stations over the western Hellenic arc, we were able to locate earthquakes with an accuracy better than 5 km, both in epicentre and depth. The accuracy of the locations and the large number of fault plane solutions allow us to get a tectonic image complementary to that obtained from strong earthquakes. The highest seismicity is seen along the Hellenic arc and located in places where changes in the bathymetry are seen. In the western Peloponnese we mapped compression where neotectonic studies show extension; we also located earthquakes within the lower crust, which is rather unusual and suggest that there is a relation between the strain level and the brittle deformation.

Our ability to compute 80 fault plane solutions in a small area allows us to map a heterogenous strain field in the western Hellenic arc, different from neotectonic observa-

tions. We observe compression in the western Peloponnese which rotates from NE–SW to E–W; in the northern Peloponnese the extension is oriented N–S and rotates counterclockwise to become E–W in the Kythira strait.

The observed strain field is likely to be due to the superposition of the one due to the spreading of Aegea and to the other due to the collision against Apulia which behaves as an indenter. This collision could explain both the crustal thickening observed in Northern Peloponnese and Epirus as the deepening of the brittle–ductile transition.

ACKNOWLEDGMENTS

We would like to thank all the observers who helped us in maintaining the network: S. Agellis, C. Anagnostou, M. Balaktsi, N. Gegas, K. Griga, P. Krana, G. Michalettos, M. Papachristou, N. Papadimitriou, N. Papanagnou, J. Papastamatiou, A. Paul, M. Poultsidis, D. Sarafis, L. Scordilis, A. Simonin, K. Tamisoglou, A. Tsagarakis, I. Venizelos, Th. Vourakis. D. Panagiotopoulos, M. Scordilis, N. Delibasis, J. Baskoutas took part of the responsibility in organizing the field work. This experiment would not have been possible without the important contribution of I. Latousakis and M. Frogneux, and without the encouragements of B. Papazachos and I. Drakopoulos. We benefited from interesting discussions with P. Molnar who reviewed several versions of the manuscript. J. Jackson and C. Laj suggested improvements to the original manuscript. L. Jenatton and S. Perrier helped in processing the data, J. Blanchet and INSU helped in the bureaucracy. This work has been supported by EEC, Stimulation Contract #121.

REFERENCES

Ambraseys, N. N., 1981. On the long term seismicity of the Hellenic arc, *Boll. Geof. Teor. Appl.*, **XXIII,** 355–359.

Anderson, H. & Jackson, J., 1987. Active tectonics of the Adriatic region, *Geophys. J. R. astr. Soc.*, **91,** 937–983.

Angelier, J., 1979. Néotectonique de l'arc égéen, *Soc. Géol. du Nord,* **3,** 418.

Angelier, J., Lyberis, N., Le Pichon, X., Barrier, E. & Huchon, P., 1982. The neotectonic development of the Hellenic Arc and the Sea of Crete: a synthesis, *Tectonophysics,* **86,** 159–196.

Aubouin, J., 1959. Contribution à l'étude géologique de la Grèce septentrionale: les confins de l'Epire et de la Thessalie, *Ann. Géol. Pays Hell.*, **10,** 525p.

Bath, M., 1982. Seismic energy mapping applied to Sweden, *Tectonophysics,* **81,** 85–98.

Brooks, M. & Ferentinos, G., 1984. Tectonics and sedimentation in the Gulf of Corinth and Zakynthos and Kefallinia channels, western Greece, *Tectonophysics,* **101,** 25–54.

Brooks, M., Clews, J. E., Melis, N. S. & Underhill, J. R., 1988. Structural development of Neogene basins in western Greece, *Basin Res.*, **1,** 129–138.

Célérier, B., 1988. How much does slip on a reactivated fault plane constrain the stress tensor? *Tectonics,* **7,** 1257–12778.

Chen, W. P. & Molnar, P., 1983. Focal depth of intracontinental and intraplate earthquakes and their implications for the thermal and mechanical properties of the lithosphere, *J. geophys. Res.*, **88,** 4183–4214.

Comninakis, P. E. & Papazachos, B. C., 1986. A catalogue of earthquakes in Greece and surrounding area for the period 1901–1985, *Pub. Lab. Univ. Thessaloniki,* vol. 1.

Doudsos, T., Kontopoulos, N. & Ferentinos, G., 1985. Das westliche Ende des Korinth Graben, *N. Jb. Geol Paläont. Mh. H.*, **11,** 652–666.

Doudsos, T., Kontopoulos, N. & Frydas, D., 1987. Neotectonic evolution of northwestern continental Greece, *Geologishe Rundschau,* **76,** 433–450.

England, P., Houseman, G. & Sonder, L., 1985. Length scales for continental deformation in convergent, divergent, and strike-slip environments: analytical and approximate solutions for a thin viscous sheet model, *J. geophys. Res.*, **90,** 3551–3557.

Ferentinos, G., Brooks, M. & Doudsos, T., 1985. Quaternary tectonics in the Gulf of Patras, western Greece, *J. struct. Geol.*, **7,** 713–717.

Grange, F., Hatzfeld, D., Cunningham, P., Molnar, P., Roecker, S. W., Suarez, G., Rodrigues, A. & Ocola, L., 1984. Tectonic implications of the microearthquake seismicity and fault plane solutions in Southern Peru, *J. geophys. Res.*, **89,** 6139–6152.

Hatzfeld, D., Christodoulou, A. A., Scordilis, E. M., Panagiotopoulos, D. & Hatzidimitriou, P. M., 1986. A microearthquake study of the Mygdonian graben (northern Greece), *Earth planet. Sci. Lett.*, **81,** 379–396.

Hatzfeld, D. *et al.*, 1989. The Hellenic subduction beneath the Peloponnese, first results of a microearthquakes study, *Earth. planet. Sci. Lett.*, **93,** 283–291.

Hatzidimitriou, P. M., 1984. Seismogenic volumes and seismic sources of the Aegean and surrounding areas, *PhD thesis,* University of Thessaloniki.

Houseman, G. & England, P., 1986. Finite strain calculations of continental deformation 1. Method and general results for convergent zones, *J. geophys. Res.*, **91,** 3651–3663.

Jackson, J. & McKenzie, D., 1988. The relationship between plate motion and seismic moment tensors, and the rates of active deformation in the Mediterranean and Middle East, *Geophys. J.*, **93,** 45–73.

Jackson, J., Fitch, T. J. & McKenzie, D. P., 1981. Active thrusting and the evolution of the Zagros fold belt, in *Trust and Nappe Tectonics,* pp. 371–379, eds McClay, K. R. & Price, N. J., Geological Society of London.

Jackson, J., Gagnepain, J., Houseman, G., King, G. C. P., Papadimitriou, P., Soufleris, C. & Virieux, J., 1982. Seismicity, normal faulting and the geomorphological development of the Gulf of Corinth (Greece): The Corinth earthquake of February 1981, *Earth planet. Sci. Lett.*, **57,** 377–397.

Karakostas, B. G., 1988. Relationship between the seismic activity and geological and geomorphological feature of the Aegean and the surrounding areas, *PhD thesis,* University of Thessaloniki.

King, G. C. P., Ouyand, Z., Papadimitriou, P., Deschamps, A., Gagnepain, J., Houseman, G., Jackson, J., Soufleris, C. & Virieux, J., 1985. The evolution of the Gulf of Corinth (Greece): an aftershock study of the 1981 earthquakes, *Geophys. J. R. astr. Soc.*, **80,** 677–693.

Lallemant, S., Lyberis, N. & Thiebault, F., 1983. Le décrochement nord-Maniote: une structure transverse de l'arc égéen externe en Péloponnèse méridional (Grèce), *C. R. Acad. Sci. Paris,* **296,** 1545–1550.

Lee, W. H. K. & Lahr, J. C., 1972. Hypo71 (revised), a computer program for determining hypocenters, magnitude and first motion pattern of local earthquakes, *US Geological Survey Open File Report 75–311.*

Le Pichon, X. & Angelier, J., 1979. The Hellenic arc and trench system: a key to the neotectonic evolution of the Eastern Mediterranean area, *Tectonophysics,* **60,** 1–42.

Le Pichon, X., Lyberis, N., Angelier, J. & Renard, V., 1982. Strain distribution over the east Mediterranean ridge, a synthesis incorporating new Sea-Beam data, *Tectonophysics,* **86,** 243–274.

Le Quellec, P. & Mascle, J., 1979. Hypothèse sur l'origine des

Monts Matapan (marge ionienne du Péloponnèse), *C. R. Acad. Sci. Paris*, **288**, 31–34.

Le Quellec, P., Mascle, J., Got, H. & Vittori, J., 1980. Seismic structure of Southwestern Peloponnese Continental Margin, *A.A.P.G. Bull.*, **64**, 242–263.

Le Quellec, P., Mascle, J., Got, H., Vittori, J. & Mirabile, L., 1979. Esquisse structurale de la marge continentale dans le sud du Péloponnèse, *C. R. Somm. Soc. Géol. Fr.*, **2**, 76–79.

Leydecker, G., Berckhemer, H. & Delibassis, N., 1978. A study of seismicity in the Peloponnese Region by precise hypocenter determinations, in *Alps, Appenines, Hellenides*, pp. 406–410, eds Closs, H., Roeder, D. & Schmidt, K., Verlagsbuchhandlung, Stuttgart.

Lyberis, N. & Lallemant, S., 1985. La transition subduction–collision le long de l'arc égéen externe, *C. R. Acad. Sci. Paris*, **17**, 885–890.

Lyberis, N., Lallemant, S. & Thiebault, F., 1983. La structure transverse Nord-Maniote et la déformation (depuis le Miocène supérieur) du Péloponnèse dans le cadre de l'arc égéen externe, *Ann. Soc. Géol. Nord*, **TCIII**, 273–283.

Lyberis, N., Angelier, J., Barrier, E. & Lallemant, S., 1982. Active deformation of a segment of arc, the strait of Kythira, Hellenic arc, Greece, *J. struct. Geol.*, **4**, 299–311.

Lyon-Caen, H. *et al.*, 1988. The 1986 Kalamata (south Peloponnesus) earthquake: detailed study of a normal fault, evidences for east–west extension in the Hellenic arc, *J. geophys. Res.*, **93**, 14 967–15 000.

Makris, J., 1978. The crust and upper mantle structure of the Aegean region from deep seismic soundings, *Tectonophysics*, **46**, 269–284.

Makropoulos, K., 1978. The statistics of large earthquake magnitude and an evaluation of Greek seismicity, *PhD thesis*, Edinburgh University.

Makropoulos, K. C. & Burton, P. W., 1981. A catalogue of seismicity in Greece and adjacent areas, *Geophys. J. R. astr. Soc.*, **65**, 741–762.

Martin, C., 1988. Géométrie et Cinématique de la subduction égéenne, structure en vitesse et en atténuation sous le Péloponnèse, *Thèse*, Université Joseph Fourier, Grenoble.

McKenzie, D., 1969. The relation between fault plane solutions for earthquakes and the directions of the principal stresses, *Bull. seism. Soc. Am.*, **59**, 591–601.

McKenzie, D., 1972. Active tectonics of the Mediterranean region, *Geophys. J. R. astr. Soc.*, **30**, 109–185.

McKenzie, D., 1978. Active tectonics of the Alpine–Himalayan Belt: the Aegean Sea and surrounding regions, *Geophys. J. R. astr. Soc.*, **55**, 217–254.

Melis, N. S., Brooks, M. & Pearce, R. G., 1989. A microearthquake study in the Gulf of Patras region, western Greece, and its seismotectonic interpretation, *Geophys. J. R. astr. Soc.*, **98**, 515–523.

Mercier, J. L., 1981. Extensional–compressional tectonics associated with the Aegean Arc: comparison with the Andean Cordillera of South Peru–North Bolivia, *Phil. Trans. R. Soc. Lond.*, A, **300**, 337–355.

Mercier, J. L., Sorel, D. & Simeakis, K., 1987. Changes in the state of stress in the overriding plate of a subduction zone: the Aegean Arc from the Pliocene to the Present, *Ann. Tectonicae*, **1**, 20–39.

Mercier, J. L., Delibassis, N., Gauthier, A., Jarrige, J. J., Leureille, F., Philip, P., Sébrier, M. & Sorel, D., 1979. La néotectonique de l'arc égéen, *Rev. Géol. Dyn. Géogr. Phys.*, **21**, 67–92.

Merle, O., 1989. Strain models within spreading nappes, *Tectonophysics*, **165**, 57–71.

Minster, J. B. & Jordan, T. H., 1978. Present day plate motions, *J. geophys. Res.*, **83**, 5331–5354.

Panagiotopoulos, D. G. & Papazachos, B. C., 1985. Travel times of Pn waves in the Aegean and surrounding area, *Geophys. J. R. astr. Soc.*, **80**, 165–176.

Papazachos, B. C. & Comninakas, P. E., 1971. Geophysical and tectonic features of the Aegean Arc, *J. geophys. Res.*, **76**, 8517–8533.

Papazachos, B. C. & Comninakis, P. E., 1982. Long term earthquake prediction in the Hellenic trench arc system, *Tectonophysics*, **86**, 3–16.

Papazachos, B. C., Kiratzi, A. A., Hatzidimitriou, P. M. & Rocca, A. Ch., 1984. Seismic faults in the Aegean area, *Tectonophysics*, **106**, 71–85.

Papazachos, B. C., Kiratzi, A., Karacostas, B., Panagiotopoulos, D., Scordilis, E. & Mountrakisa, D. M., 1988. Surface fault traces, fault plane solution and spatial distribution of the aftershocks of the September 13, 1986 earthquake of Kalamata (southern Greece), *Pure appl. Geophys.*, **126**, 55–68.

Pedotti, G., 1988. Etude sismotectonique du Péloponnèse et réponse sismique d'une vallée sédimentaire en Grèce du Nord, *Thèse*, Université Joseph Fourier, Grenoble.

Scordilis, E. M., Karakaisis, G. F., Karakostas, B. C., Panagiotopoulos, D. G. & Papazachos, B. C., 1985. Evidence for transform faulting in the Ionian Sea: The Cephalonia Island earthquake sequence of 1983, *Pageoph.*, **123**, 387–397.

Sébrier, M., 1977. Tectonique récente d'une transversale à l'arc égéen, *Thèse de spécialité*, Université d'Orsay.

Sibson, R. H., 1984. Roughness at the base of the seismogenic zone: contribution factors, *J. geophys. Res.*, **89**, 5791–5799.

Sorel, D., 1976. Etude néotectonique dans l'arc égéen externe occidental; les îles ioniennes de Kephallina et Zakinthos et l'Elide occidentale, *Thèse de spécialité*, Université d'Orsay.

Taymaz, T., 1989. Source parameters of large earthquakes near Crete, *Terra Abstract*, p. 110, V EUG Meeting, Strasbourg.

Tozzi, M., Kissel, C., Funiciello, R., Laj, C. & Parotto, M., 1988. A clockwise rotation of southern Apulia? *Geophys. Res. Lett.*, **15**, 685–688.

Wyss, M. & Baer, M., 1981. Earthquake hazard in the Hellenic arc, in *Earthquake Prediction*, Maurice Ewing Series, vol. 4, pp. 153–172, American Geophysical Union, Washington, DC.

APPENDIX

Lower hemisphere focal spheres of the crustal earthquakes. Black and empty dots are reliable compressional and dilational first motions, + and − are uncertain.

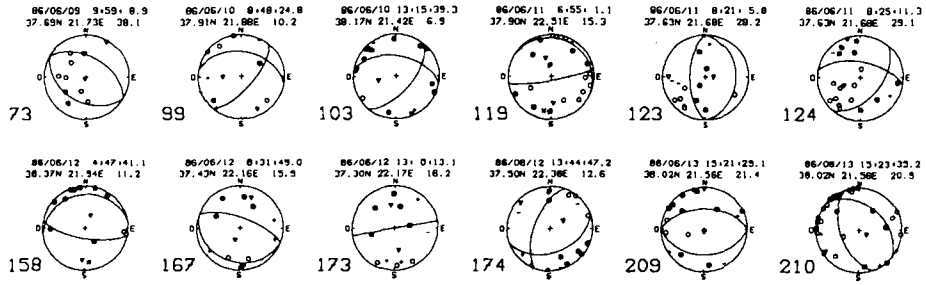

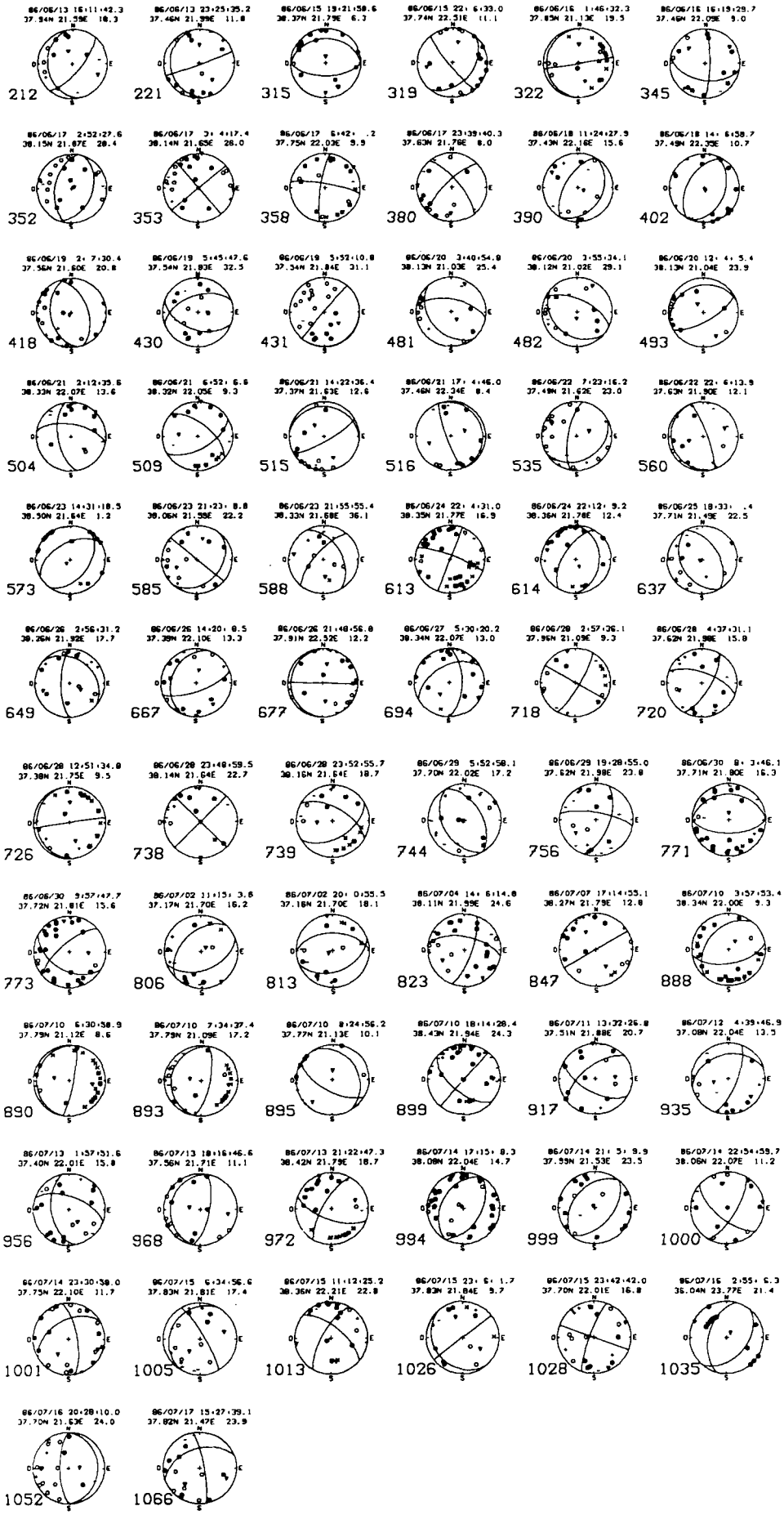
212
221
315
319
322
345
352
353
358
380
390
402
418
430
431
481
482
493
504
509
515
516
535
560
573
585
588
613
614
637
649
667
677
694
718
720
726
738
739
744
756
771
773
806
813
823
847
888
890
893
895
899
917
935
956
968
972
994
999
1000
1001
1005
1013
1026
1028
1035
1052
1066

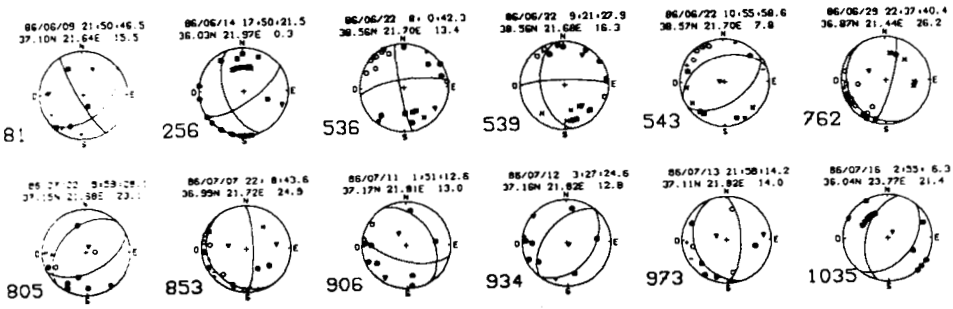
86/06/09 21:50:46.5
37.10N 21.64E 15.5
81
86/06/14 17:50:21.5
36.03N 21.97E 0.3
256
86/06/22 8: 0:42.3
38.56N 21.70E 13.4
536
86/06/22 9:21:27.9
38.56N 21.68E 16.3
539
86/06/22 10:55:58.6
38.57N 21.70E 7.8
543
86/06/29 22:37:40.4
36.87N 21.44E 26.2
762
86/07/07 22: 8:43.6
36.99N 21.72E 24.9
853
86/07/11 1:31:12.6
37.17N 21.81E 13.0
906
86/07/12 3:27:24.6
37.18N 21.82E 12.8
934
86/07/13 21:38:14.2
37.11N 21.82E 14.0
973
86/07/16 2:55: 6.3
36.04N 23.77E 21.4
1035